CHARACTERISTICS OF STREAM SOURCE WATER CONTRIBUTIONS AND ASSOCIATED GEOCHEMICAL SIGNATURES ALONG A CLIMATE AND VEGETATION GRADIENT IN A GLACIERIZED LANDSCAPE, SOUTHCENTRAL ALASKA

by

Hannah K. Richardson

A thesis

submitted in partial fulfillment

of the requirements for the degree of

Master of Science in Geoscience

Boise State University

August 2023

BOISE STATE UNIVERSITY GRADUATE COLLEGE

DEFENSE COMMITTEE AND FINAL READING APPROVALS

of the thesis submitted by

Hannah K. Richardson

Thesis Title:	Characteristics of Stream Source Water Contributions and Associated Geochemical Signatures Along a Climate and Vegetation Gradient in a Glacierized Landscape, Southcentral Alaska.
Date of Final Oral Examination:	12 April 2023

The following individuals read and discussed the thesis submitted by student Hannah K. Richardson, and they evaluated the student's presentation and response to questions during the final oral examination. They found that the student passed the final oral examination.

Anna Bergstrom, Ph.D.	Chair, Supervisory Committee
Joshua Koch, Ph.D.	Member, Supervisory Committee
Kendra E. Kaiser, Ph.D.	Member, Supervisory Committee
Ellyn Enderlin, Ph.D.	Member, Supervisory Committee

The final reading approval of the thesis was granted by Anna Bergstrom, Ph.D., Chair of the Supervisory Committee. The thesis was approved by the Graduate College.

DEDICATION

This thesis is dedicated to all of those who supported me most during my Boise chapter. I could not have been as successful without the support of Hadley Reine, who cared for me when I didn't have the energy to take care of myself. Thank you to Ali Belzer and Sarah Halperin for keeping me active, well-fed, and loved. Thank you to my department community for all the shared lunches in which we could commiserate together. I also could not have started this journey without the mentorship of Kena Fox-Dobbs or Anne Fetrow. I also dedicate this to my parents, who have always encouraged me to pursue a higher degree in science.

ACKNOWLEDGMENTS

I would like to acknowledge the support I received to make this thesis possible, including an NSF Earth Sciences Post-Doctoral Fellowship awarded to Dr. Anna Bergstrom, the Marie Morisawa Research Award, and the Burnham Award. I would like to thank all who helped with field data collection: Zan Fredrick, Emily Baker, and James Shanley. I would also like to thank those who helped me process samples in the lab: Mac Beers and Bryn Chaffee. Research could not have been possible without the help of Alpine Air Alaska and the USGS.

ABSTRACT

Mountain-derived snow and ice melt are essential for global water resources, and over one-sixth of the population depends on melt for freshwater. Rising air temperatures are causing vegetation to replace snow- and ice-covered landscapes and precipitation regimes to change. Collectively, these changes will alter the hydrology of mountain environments, although the exact impacts to hydrologic regimes are poorly understood. The source waters of streamflow (i.e. the proportion of ice melt, snowmelt, rain, and groundwater) dictate the timing and magnitude and affect temperature, sediment, and nutrient fluxes. By examining differences in source waters across basins with varying land covers and precipitation regimes, we can better predict the impact warming temperatures may have on streamflow from both a physical and biogeochemical perspective. Glaciers also physically weather their environment, which increases chemical weathering potential. High chemical weathering rates can impact global carbon cycling, but the extent and net influence of their impact is unknown. This thesis examines shifting source water contributions and chemical weathering patterns in sub-watersheds of the Nellie Juan basin on the Kenai Peninsula in Southcentral Alaska that range in percent glacier cover, elevation, and land cover type. To do so, a variety of geochemical, remote sensing, and modeling techniques were used. I found strong relationships between elevation, source water contributions, and land cover. There were also clear differences in the timing of snow and ice melt contributions to streams between glacierized and non-glacial streams. Groundwater is shown to be a major contributor to streamflow across the

basin and may become increasingly important as snowpack and glacier melt decrease. Geochemical analyses show that the main driver of weathering-derived solutes in the region is bedrock type and that the presence of the glacier seems to play only a minor role in weathering. I also find a positive relationship between the proportion of groundwater in streamflow and weathering-derived solutes. This research characterizes the shift from a glacial to a deglaciated landscape through the lens of source water contribution and geochemical weathering regimes. Broadly, these findings can help improve our understanding of how water resources, biogeochemical fluxes, and carbon cycling in glacierized basins are impacted by warming air temperatures.

TABLE OF CONTENTS

LIST OF TABLES

LIST OF FIGURES

LIST OF PICTURES

LIST OF ABBREVIATIONS

EC	Electrical Conductivity
NJ	Nellie Juan
LIA	Little Ice Age
HDPE	High Density Poly Ethylene
ET	Evapotranspiration
DI	De-Ionized
ICP-MS	Inductively Coupled Plasma Mass Spectrometry
USGS	United States Geological Survey

CHAPTER ONE: INTRODUCTION

Glacier melt and seasonal snowmelt provides freshwater resources to over a billion people and supports downstream ecosystems from rivers to nearshore marine environments (Viviroli et al., 2007; Barnett et al., 2005; Milner et al., 2017; Milner et al., 2009). Humans depend on meltwater for services such as energy production, tourism, and agricultural water supply (Milner et al., 2017). More indirectly, humans benefit economically and culturally from fish like Pacific Salmon (*Oncorhynchus* spp.) that rely on glacier- and snowmelt-dominated streams (O'Neel et al., 2015; Milner et al., 2009; Milner et al., 2017). The resources that glacier and snowmelt provide will be impacted as melt quantity and timing change.

Warming air temperatures are changing the hydrology of snow- and ice-dominated regions (Barnett et al., 2005). Glaciers are losing mass worldwide, with some of the highest losses observed in coastal Alaska (Hugonnet et al., 2021; Gardner et al., 2013). The concept of "peak water" describes the maximum amount of glacial meltwater (Gleick and Palanaippan, 2010). Glaciers recede to a point where they contribute less to streamflow and it is estimated that about half of the world's glaciers have passed peak water (Huss and Hock, 2018). Warming air temperatures also decrease total annual snowpack depth and cause melt to occur earlier in the year (Mote et al., 2005; Barnett et al., 2005). Snowpack depth is particularly sensitive in temperate climates, such as those in Coastal Alaska, as only a few degrees of warming can change the phase of precipitation from snow to rain (Mote et al., 2005). Global climate change is causing

complex hydrologic changes in glacierized and snowmelt-dominated regions which influence the physical hydrology of streams.

Stream temperature, magnitude, and timing are all driven by ice and snowmelt timing (Milner et al., 2009). Earlier seasonal snowmelt is slower than late-season melt, resulting in earlier contributions to streamflow and reduced peak discharge (Musselman et al., 2017). Longer and hotter summer seasons coupled with less snow on the landscape will increase the potential for glacier melt for the glaciers that have not yet reached peak water, which will in turn increase peak flow (O'Neel et al., 2014; Hannah et al., 2000). Although the physical aspects of glacier and snowmelt-dominated hydrology are well studied, the transition from a glacier-dominated to a snowmelt-dominated watershed is poorly understood. By examining the transition from a glacier to a snowmelt-dominated watershed, we can better understand the biogeochemical impacts of such a change.

Glaciers influence the biogeochemistry of downstream hydrologic systems by altering nutrient and sediment fluxes (Hood and Berner, 2009; Milner et al., 2009; Milner et al., 2017). For example, glaciers are a source of highly labile dissolved organic carbon that drives downstream food webs (Milner et al., 2017; Fellman et al., 2015; Hood and Berner, 2009). High sediment loads mobilized by glaciers limit primary productivity, such that decreases in glacier melt will alter the transformation of organic matter (Milner et al., 2017). Carbon and nitrogen concentrations are lower in glacial streams as compared to streams that flow through vegetated soils, while phosphorus concentrations are higher (Hood and Berner, 2009). Although the biogeochemical signatures of individual steam source waters (i.e. glacier melt, snowmelt, groundwater) are well

understood, the combined impact on downstream ecosystems cannot be assessed without an understanding of the way these source waters are partitioned.

Chemical weathering rates are enhanced in regions of high physical weathering, meaning that glaciers may play a significant role in the global carbon cycle. To assess the impact glaciers have on the global carbon cycle, we need to understand the type of chemical weathering processes occurring. Atmospheric CO_2 consumption is driven by silica weathering rates, while carbonate weathering supplies CO_2 to the atmosphere when driven by sulfuric acid production by pyrite oxidation (Berner and Maasch, 1996; Walker et al., 1981; Torres et al., 2017). Previous studies have shown that the physical erosion of glaciers may increase silicate weathering rates and thus the production of alkalinity (Herman et al., 2013; Foster and Vance, 2006), while others have shown that cold temperatures limit silicate weathering in glacierized regions, decreasing the production of alkalinity (Kump et al., 1999). Carbonate weathering by sulfide oxidation, which produces CO_2, is not limited by temperature and is present to some degree in all lithologies (White et al., 1999; White and Brantley 2003). Glaciers have been shown to weather significant quantities of carbonates due to the presence of fresh sediment (Anderson et al., 2000). The net influence of glaciation on the global carbon cycle is unknown, and more research regarding silicate and carbonate weathering patterns in glacierized basins is needed to understand the impact of glaciers on the global carbon cycle.

This research is conducted in the Nellie Juan basin, located on the Kenai Peninsula of southcentral Alaska. The Nellie Juan basin is a partially glacierized catchment that is closely linked to the nearshore environment. The Nellie Juan River

drains into Prince William Sound, which is a highly productive marine environment that supports groundfish and salmon (*Oncorhynchus* spp.) fisheries (Campbell, 2018).

The Wolverine Glacier watershed lies within the northern portion of the Nellie Juan watershed and contains the Wolverine Glacier. The Wolverine Glacier is a USGS benchmark glacier that has been monitored via mass balance studies since 1966. The USGS installed a stream gauge 100 m below the glacier terminus in 1966, and the terminus has receded ~1500 m since. A strong scientific understanding of glacier change coupled with historic meteorological and discharge records make the Wolverine Glacier region an excellent candidate for studying changing hydrologic regimes. My thesis examines the Nellie Juan watershed, the Wolverine Glacier watershed, and a variety of non-glacial sub-watersheds to understand differences in physical and chemical hydrology.

This research is presented in three chapters. Chapter 2 focuses on physical differences in hydrology across a range of non-glacial and glacierized basins. Basins and sub-basins within the Nellie Juan watershed span a range of percent glacier cover, elevation range, and landscape cover, as identified using a satellite image supervised classification approach (Appendix A). Their source water contributions can be compared to elucidate the ways in which percent glacier cover, precipitation regimes, and vegetation impact streamflow contribution. I partition source waters into three categories: rain, snow/ice melt, and groundwater using a three end-member mixing model. I find that snowmelt contributes proportionally more at high elevations, which are dominated by tundra vegetation, persistent snow, and bare bedrock. Rain contributes more to low-elevation streams, which are dominated by forests. I additionally find that groundwater is

an important contributor to flow in all streams, but particularly in low-elevation streams and during the spring and fall seasons. This indicates the importance of groundwater in mountain systems and better characterizes the interactions between source waters in different climatic and vegetative regimes.

Chapter 3 examines the type of chemical weathering occurring in the Nellie Juan watershed. I use a synoptic sampling campaign across three non-glacial streams that pass over a Little Ice Age (LIA) trimline, in addition to an analysis of historic glacierized and non-glacial geochemical datasets from streams in the Nellie Juan basin. A suite of ion, nutrient, and isotopic data are used to examine relationships across and between streams. I find that bedrock type plays the largest role in determining geochemical weathering signatures, and that the relative contribution of groundwater increases weathering-derived solutes. I also find that the presence of the glacier and glacial features do not impact weathering signatures. These findings have implications for both the scale at which chemical weathering occurs and the importance of groundwater in weathering processes and solute generation. Broadly, this research contributes to knowledge regarding glacial influence on global carbon fluxes.

Chapter 4 summarizes the connections between the previous chapters, which examine both the physical and chemical changes that are occurring in rapidly changing glacial environments. As glaciers continue to recede, precipitation regimes change, and vegetation encroaches and becomes denser, there will be physio-chemical changes to hydrologic systems. This work is unique in that it encompasses the interactions between non-glacial hillslope processes, groundwater, and glacier melt to connect concepts in mountain hydrology to glacial hydrology.

CHAPTER TWO: WARMING INDUCED CHANGES IN STREAM SOURCE WATER CONTRIBUTION AND VEGETATION COVER IN GLACERIZED BASINS

1. Introduction

Alaska's air temperatures have risen more than 2°C since 1950, a much faster rate than the rest of the Northern Hemisphere (Walsh and Brettschneider, 2019). Warming temperatures are melting glaciers at some of the highest rates in the world (Hugonnet et al., 2021; Gardner et al., 2013; O'Neel et al., 2015) and causing precipitation trends to change (McAfee et al., 2014). Additionally, vegetation is shifting in distribution and density as the growing season elongates and more ice-free surfaces are exposed (Littell et al., 2018; McAfee et al., 2014; Dial et al., 2007). Combined increases in glacier melt, changes in precipitation regimes, and new vegetation patterns may result in new hydrologic and biogeochemical regimes (Adam et al., 2009; Curran and Biles, 2021; Hammond et al., 2019; Foks et al., 2018).

Multiple water sources that contribute to streams in glacierized watersheds, and downstream ecosystems rely on the unique timing and physical and biogeochemical properties of each source. Streams are driven by a combination of rain, snow, ice, and groundwater in glacierized basins. Snowmelt is driven by air temperature and solar radiation and occurs over a period of multiple months in watersheds with a large elevation range (Curran and Biles, 2021; Lundquist et al., 2004). Glacial melt is also driven by air temperature and solar radiation but occurs after snow on the glacier surface

has melted and peak flows occur in response to maximum summer temperatures (Hock, 2005). Glaciers have been shown to play an important role in downstream ecosystems by contributing to colder stream temperatures, higher levels of specific conductivity, increased turbidity, and labile carbon fluxes (Hood and Berner, 2009; Kneib et al., 2020, Milner et al., 2017). Rain events increase in frequency in the late summer and fall resulting in an event-based hydrograph, which flushes and mobilizes terrestrial solutes and nutrients (Curran and Biles, 2021; Bergstrom et al., 2021; Hood and Berner, 2009).

Stream source water contributions are shifting as precipitation form and timing respond to warming temperatures. Snowmelt contributions are decreasing as precipitation that historically fell as snow instead falls as rain in response to warming winter and spring temperatures (Littell et al., 2018; Walsh and Brettschneider, 2019). Warmer temperatures are additionally affecting snowpacks by causing more rain on snow events and earlier and slower spring snowmelt (Barnett et al., 2005; Musselman et al., 2017). Shifts in precipitation type and timing will impact streamflow timing and magnitude, as well as groundwater recharge rates.

Glacial melt contribution to streamflow will decrease after reaching “peak water”, or the maximum contribution of ice to streamflow (Gleick and Palaniappan, 2010; Huss and Hock, 2018). Peak water has passed for about half of the world’s glaciers, while the other half are estimated to reach peak water by the end of the century (Huss and Hock, 2018). As basins become deglaciated and melt contributes less to streamflow, streams will become increasingly driven by precipitation inputs. The transition from a glacially-driven to a precipitation-driven watershed is poorly understood from a hydrologic perspective (Kyle and Brabets, 2001; Neal et al., 2002; Collins et al., 2006). An

understanding of source water contribution to streamflow in glacierized and non-glacial basins is needed to better predict the changing hydrology of this region.

Geochemical signatures of source waters have been used in many studies to partition stream source waters (Frisbee et al., 2011; Liu et al., 2004; Koch et al., 2014). Snow or ice and rain are commonly distinguished using $\delta^{18}O$, as rain is more enriched in $\delta^{18}O$ relative to snow/ice (Dansgaard, 1964; Beria et al., 2018). Groundwater has high solute concentrations due to subsurface weathering processes, and electrical conductivity (EC) is often used to distinguish meteoric water from groundwater (Scribner et al., 2015; Frisbee et al., 2011). Relationships between EC and $\delta^{18}O$ can be leveraged using a mixing model to determine the proportion of source waters in streamflow.

In this paper, I make use of the unique EC and $\delta^{18}O$ signatures of glacier and snowmelt, precipitation, and groundwater to address the following question: how does stream source water contribution vary spatially and temporally along glacierized and off-glacier streams? To do so, I examine a series of sub-watersheds that range in percent glacier cover from 0-60%. I additionally isolate non-glacial watersheds across an elevation gradient to assess the impact of precipitation phase on streamflow. A three end-member mixing model is used to partition source waters using EC and $\delta^{18}O$ as tracers. These results help us better understand the hydrologic changes deglaciating basins may exhibit in response to warming temperatures.

2. Methods

2.1 Study Site

I conducted research in the Nellie Juan watershed located in south central Alaska on the Kenai Peninsula, between Cook Inlet and the Gulf of Alaska. The Nellie Juan

River watershed is 450 km^2 and has ~40% glacier cover (Bergstrom et al., 2021). The elevation of the watershed ranges from 0-1,562 m. The Nellie Juan River, which begins at Nellie Juan Lake, empties into Kings Bay which in turn connects to Prince William Sound (Figure 2.1). A stream gauge on the Nellie Juan River was operational between 1961 to 1965 and measured an average discharge of 24 $m^3\ s^{-1}$ (Bergstrom et al., 2021). The Nellie Juan watershed is characterized by a maritime climate, with warmer and wetter conditions than continental climates. The mean annual temperature is -0.2°C and precipitation exceeds 3 m/year with about 60-70% falling as snow, as indicated by a USGS meteorological station located at 990 m above sea level in the northern portion of the watershed (O'Neel et al., 2019; Bergstrom et al., 2021, Figure 2.2).

The Nellie Juan watershed spans rock and ice-covered alpine landscapes to coastal forests. The highest elevations are dominated by alpine tundra vegetation with a series of small streams and lakes flowing towards, and in some cases, under adjacent glaciers. At mid-elevation, the landscape is dominated by successional shrubs such as alder (*Alnus* spp.) and willow (*Salix* spp.). Spruce (*Picea* spp.) forests dominate low elevations. Soils at high elevations are classified as Cryod-Cryorthent type and are typically shallow, acidic, rich in fragmented rock, and well drained (van Patten, 2000). Low elevation soils are classified as Kasitna-Tutka soils, typically loamy, well drained, and supportive of Sitka spruce forests (Van Patten, 2000). Regional bedrock is classified as part of the Valdez group, consisting of metasedimentary graywacke, siltstone, and shale (Wilson et al., 2012).

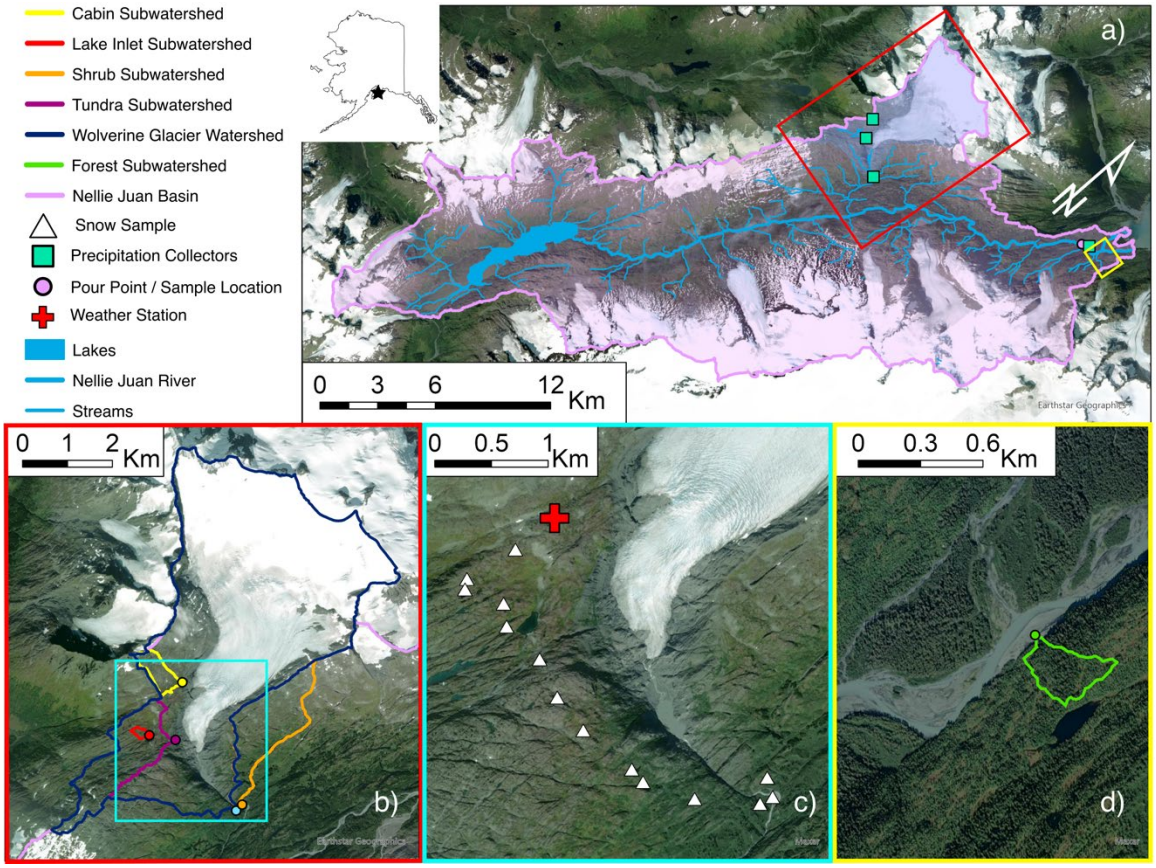

Figure 2.1. Site map of a) the entire Nellie Juan basin outlined and shaded in pink, and the Wolverine Glacier watershed in dark blue. The Nellie Juan River drains into Kings Bay, just visible on the right-hand side. The red box indicates the location of the subset map b), which contains four non-glacial sub-watersheds within or near the Wolverine Glacier watershed. The cyan box indicates the location of subset map c), in which snow sampling locations are marked by a white triangle and the weather station is marked by a red cross. The yellow box in panel a) indicates the subset map in d) which shows the location of the fifth non-glacial watershed near Kings Bay.

One glacierized sub-watershed (Figure 2.1a) and five non-glacial sub-watersheds (Figures 2.1b and 2.1d) within the Nellie Juan basin were chosen to quantify source water contributions along an elevation and vegetation gradient and separate the influence of glaciers. I additionally quantified source water contributions within the Nellie Juan basin as a whole by sampling near the outlet of the Nellie Juan River (Figure 2.1a).

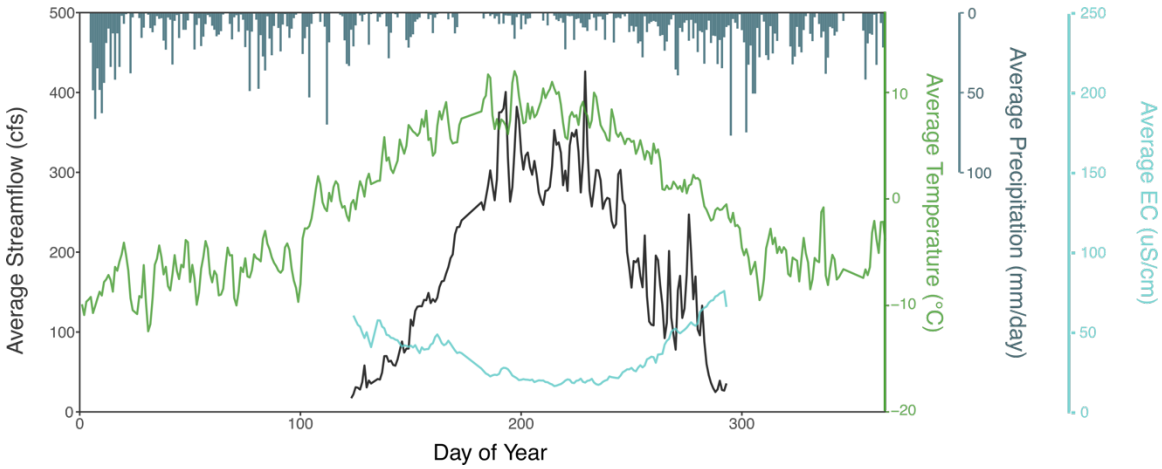

Figure 2.2. Average daily precipitation (dark blue), temperature (green), discharge (black), and EC (light blue) from the Wolverine Creek stream gage and meteorological station from 2020-2022. The stream gage is only operational during the ice-free portion of the year, leaving data gaps during the snow season.

The glacierized sub-watershed contains the Wolverine Glacier. The Wolverine Glacier watershed is a 24.6 km^2 basin with ~60% glacier cover, as delineated from a USGS-operated stream gauge on Wolverine Creek (O'Neel et al., 2019). The glacier is a USGS benchmark glacier, and mass balance studies have shown that the glacier has lost 17.1 m water equivalent from 1969 to 2018, and glacier coverage decreased from 17.1 to 15.6 km^2 (O'Neel et al., 2019). Since the installation of a stream gauge in the 1960s, the glacier terminus has receded ~1400 m. Below the Wolverine Creek stream gauge, the creek flows ~1 km before joining the Nellie Juan River (Figure 2.1a).

Three of the non-glacial sub-watersheds (Cabin, Tundra, and Lake Inlet) drain areas within the Wolverine Glacier watershed (Figure 2.1b). One (Shrub, Figure 2.1b) drains an area adjacent to the watershed and flows into Wolverine Creek just below the stream gage, while the other (Forest, Figure 2.1d) lies about 13 km northeast of Wolverine stream gage draining into the Nellie Juan River. Land cover varies across an elevational gradient in the Nellie Juan basin (see Appendix A), and the non-glacial sub-watersheds analyzed each reflects a part of the vegetation gradient observed in the region

(Figure 2.3). High-elevation sites like Lake Inlet, Cabin Stream, and Tundra Stream are primarily covered by tundra vegetation, while the mid-elevation Shrub Creek site drains a basin with a higher proportion of successional shrubs. Forest Stream drains a low-elevation forested basin.

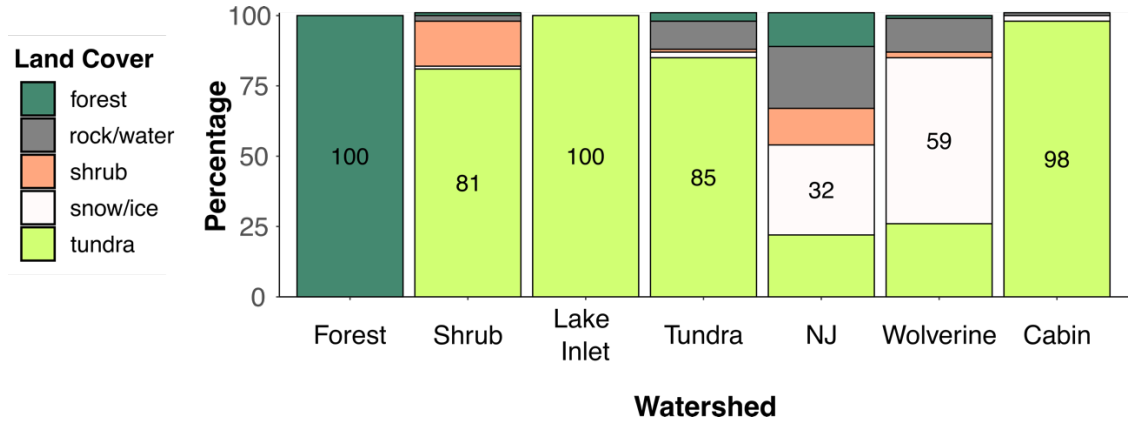

Figure 2.3. The percentage of land cover type calculated in each sub-watershed using a supervised classification. The percent coverage of the primary land cover is displayed on each bar. Each color represents the type of land cover.

2.2 Field Data Collection

This study builds upon a previously collected dataset, combining published data with our newly collected samples. Details regarding the previously collected dataset can be found in the publicly available data release (Koch et al., 2021). I collected additional stream samples from September 2021 to September 2022 at the seven sites described above (Figure 2.1). Water samples used for isotope analysis were not filtered and were collected in 30mL HDPE bottles rinsed three times and filled to minimize headspace. All samples were kept in coolers in the field to prevent unwanted freezing or warming. Samples were stored at +4°C upon returning from the field until analysis. EC data were collected using a YSI Ecosense 300 handheld probe (accuracy ±1% of reading; YSI,

2017). For water temperatures above 1.7°C, the probe automatically compensates EC to 25°C. Below 1.7°C, the following equation was used to compensate stream EC to 25°C (YSI, 2017).

$$EC_{Corrected} = \frac{EC_{Uncorrected}}{1+(0.0191*(T-25)} \quad (2.1)$$

Snowpack samples were collected in May 2022 across an elevation gradient within the Wolverine Glacier watershed (Figure 2.1c). In four snow pits, snow was collected in 10 cm increments from the snow surface to the ground surface using a 250 cm^3 wedge cutter. Ten additional snow samples were collected using a federal sampler, which collects a core extending from the surface to the base of the snowpack. All snow samples were placed directly in Zip-Lock bags upon collection. Snow was weighed to calculate density and was allowed to melt before being transferred to 30 mL HDPE bottles for isotope analysis. EC was measured from the remaining meltwater. Snow water samples were then stored in the same manner as stream water samples.

Cumulative rain samples were collected using a precipitation collector designed to minimize contact with the atmosphere and post-depositional change to the isotopic and chemical signature via evaporation as described by Gröning et al. (2012). Precipitation collectors were placed at 4 locations spanning the elevation range of the study area, located in the floodplain of the Nellie Juan River (14 m), at the Wolverine Stream gage (360 m), at the Tundra Stream monitoring location (670 m) and at the weather station (990 m; Figure 2.1). Bottles were changed every 1-2 months, whenever access to each collector was possible. Upon collection, bottles were removed from the casing and fitted with a lid. Samples were then moved to 30 mL HDPE bottles, and the remaining water was used to quantify EC.

Groundwater samples were collected at seeps in the bedrock and EC was measured to assess the source water. When EC values were over 100 μS/cm, we classified them as deep groundwater samples and collected them in the same manner as stream water. Shallow groundwater samples were collected in meadow seeps using a syringe and were classified as shallow groundwater if the EC value was under 100 μS/cm.

2.3 Laboratory Analysis

Isotope analysis was conducted using a Los Gatos Research Liquid-Water Isotope Analyzer in the Stable Isotope Laboratory at Boise State University (accuracy <± 0.12‰ for $\delta^{18}O$ and <±1.1‰ for $\delta^{2}H$, precision <± 0.25‰ for $\delta^{18}O$ and <±1.90‰ for $\delta^{2}H$). Five water standards were used spanning isotopic ranges from -6.62‰ to -37.5‰ $\delta^{18}O$ and -41.6‰ to -302.0‰ $\delta^{2}H$. Samples collected before September of 2021 were analyzed at the University of Alaska, Anchorage using a Piccaro cavity ring down spectrometer (accuracy <± 0.2‰ for $\delta^{18}O$ and <±2‰ for $\delta^{2}H$) (Koch et al., 2021).

2.4 Three End-Member Mixing Model

A three-component end member mixing model was created to determine stream source water contribution at the outlet of the seven sub-watersheds. Seasonal trends were analyzed by separating data into hydroclimatic periods, as defined by Bergstrom et al. (2021). The hydroclimatic periods describe seasonal trends and processes that are specific to streams with glacial input using relationships observed between EC and discharge. The spring melt, summer, and fall seasons were broken into four periods defined by: initial snowmelt (P1), the connection of subglacial stream networks (P2), main glacier melt (P3), and fall rains (P4). Transition dates were manually assigned for each collection year

(Table 2.1). I chose to retain the hydroclimatic periods even for non-glacially influenced streams because they serve as a useful framework to compare these results to previous data (Bergstrom et al., 2021).

Table 2.1 Day of year of hydroperiod transition. No grab sample data was collected in 2018.

Year	P1 End DOY	P2 End DOY	P3 End DOY	P4 End DOY
2016	134	166	231	281
2017	117	128	175	278
2019	139	177	229	265
2020	185	248	261	283
2021	170	235	277	
2022	142	166	215	

The three end members were rain, snow/ice, and deep groundwater. Tracers used in the model were EC and $\delta^{18}O$. EC was chosen to distinguish meteoric water from groundwater, while $\delta^{18}O$ was chosen to separate rain from snow. The model is expressed as follows:

$$1 = f_{rain} + f_{snow/ice} + f_{gw} \quad (2.2)$$

$$C_{stream} = C_{rain}f_{rain} + C_{snow/ice}f_{snow/ice} + C_{gw}f_{gw} \quad (2.3)$$

where C is the value of EC or $\delta^{18}O$ and f is the fraction of source waters: snow/ice, rain, and deep groundwater. For each location, I calculated an average EC and $\delta^{18}O$ from all

samples collected during each hydroclimatic period. Averages included all samples from 2016-2022 to allow for a higher number of samples and a representative average. Due to the relatively small amount of input data and the relatively high variability in measured end-member values, a Monte Carlo simulation was used to calculate an estimated end member signature. I randomly sampled end member EC and $\delta^{18}O$ values within one standard deviation of the mean 10,000 times. When stream samples fell within the mixing space defined by the chosen end member values, the calculated end member fractions were retained, and the average of these fractions was taken. To ensure that the mixing model performed accurately, streams with no glacial contribution were analyzed using snow values alone, while streams with a glacial contribution use a value that represents a mixed snow/ice end member.

3. Results

3.1 Source Water Signatures

Each identified end member has a unique range of $\delta^{18}O$ and EC values that can differentiate sources (Table 2.2). The range of $\delta^{18}O$ values observed in ice is similar to that seen in snowmelt, although pure snowmelt displays slightly more negative mean $\delta^{18}O$ values, such that when snow and ice melt are combined the value is more positive. Rain has more positive $\delta^{18}O$ values than snow and ice because $\delta^{18}O$ is a function of temperature (Dansgaard, 1964). All precipitation exhibits some range in the $\delta^{18}O$ space due to varying storm sources, histories, and temperatures (Dansgaard, 1964; Friedman et al., 1991; Beria et al., 2018). Groundwater has the most enriched $\delta^{18}O$ value. EC values measured for meteoric water are an order of magnitude lower than those of deep groundwater. This range fully captured the span of observed streamflow EC values.

No suitable tracers were found to distinguish shallow groundwater apart from other sources. In a $\delta^{18}O$ and EC mixing space, shallow groundwater plots within the mixing space of the other end members: rain, snowmelt, and deep groundwater (Figure 2.4). Although shallow groundwater does likely contribute to streamflow, I was unable to account for its contribution.

Table 2.2 $\delta^{18}O$ and EC values for identified end members in the Nellie Juan basin. The first number is the average of all samples collected. The standard deviation is reported in parentheses, followed by the number of samples collected.

	$\delta^{18}O$	EC
Rain	-14.47 (3.37) n=19	6.89 (5.07) n=10
Snowmelt	-17.34(2.97) n=174	2.59(1.14) n=88
Ice	-15.24 (1.57) n=460	2.46(3.08) n=22
Snowmelt and Ice	-15.82 (2.26) n= 634	2.57 (1.69) n=110
Deep Groundwater	-14.20 (1.63) n=18	149.84 (52.01) n=18
Shallow Groundwater	-14.97 (1.12) n=31	71.78 (29.57) n=23

3.2 Seasonal Trends in Off-glacier Streams

Stream values of $\delta^{18}O$ become more positive as the year progresses, ranging from values similar to snowmelt to values similar to rain (Figure 2.5, Table 2.2). EC values are generally high at the beginning and end of the sample season and are lowest mid-summer (Figure 2.5).

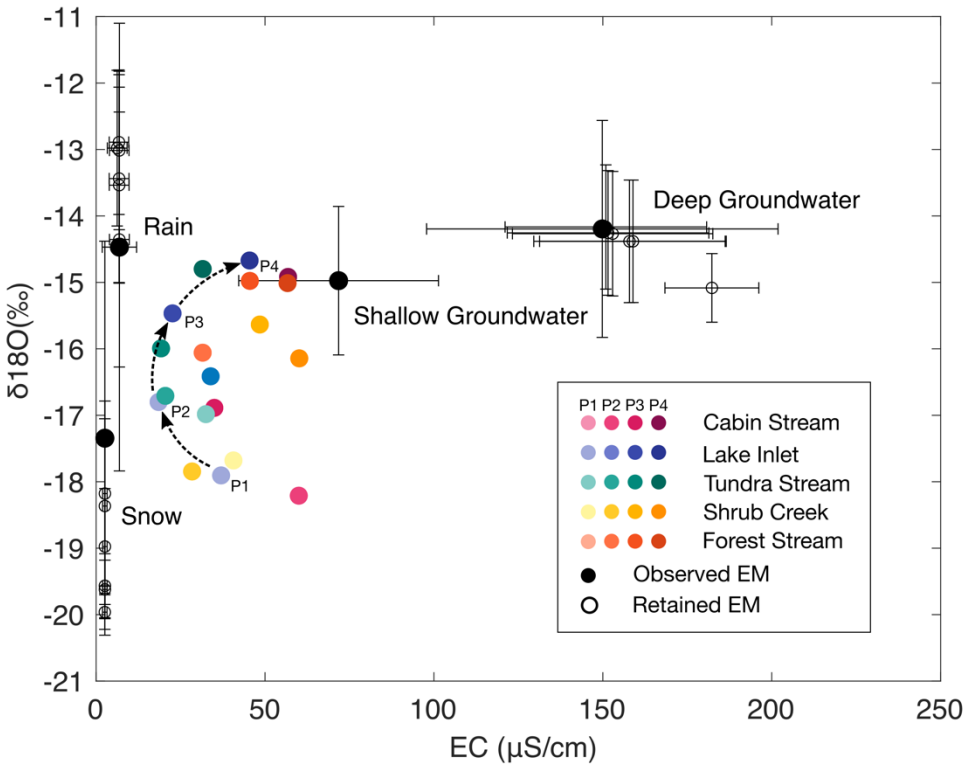

Figure 2.4. The relationship between $\delta^{18}O$ and EC in off-glacier streams and end members. Measured end members are the filled black circles, while the end member retained by the Monte Carlo simulation are the unfilled black circles. Measured stream samples are represented by filled colored circles, and the hue of each color darkens as streams move through periods 1-4. An example of a seasonal pattern of stream water chemistry is annotated by arrows connecting Lake Inlet's trend.

Mixing model results indicate that snowmelt is the dominant source of streamflow in hydroclimatic periods 1 and 2 in all off-glacier streams (Figure 2.6). All streams show a decrease in overall snowmelt contribution in the summer and fall seasons (Figures 2.4 and 2.6). Mixing model results show that snowmelt contributions range from up to 70% of streamflow in P1, to as low as 20% in P4. Rain contribution generally increases from P1 through P4. At the Cabin Stream, Lake Inlet, and Tundra Stream there are higher proportions of rain contribution in each successive period. At Shrub Creek and Forest Stream, P4 shows slightly lower rain contributions than P3. At all sites, groundwater proportions are higher in periods 1 and 4 than in periods 2 and 3.

3.3 Elevational Trends in Off-glacier Streams

Each off-glacier stream has a watershed area between 0.07 and 2.5 km^2 (Table 2.3). The mean elevation of each watershed spans a wide range; Cabin Stream has the highest mean elevation of 1206 m, and Forest Stream has the lowest mean elevation of 86 m. High-elevation watersheds have larger contributions of snowmelt, particularly in periods 1 and 2, compared to watersheds in low elevations (Figure 2.6). Larger proportions of groundwater can be found in the lower Shrub Creek and Forest Stream watersheds. However, the highest elevation Cabin Stream had some of the largest groundwater proportions. There were no strong elevational trends in rain contribution to flow.

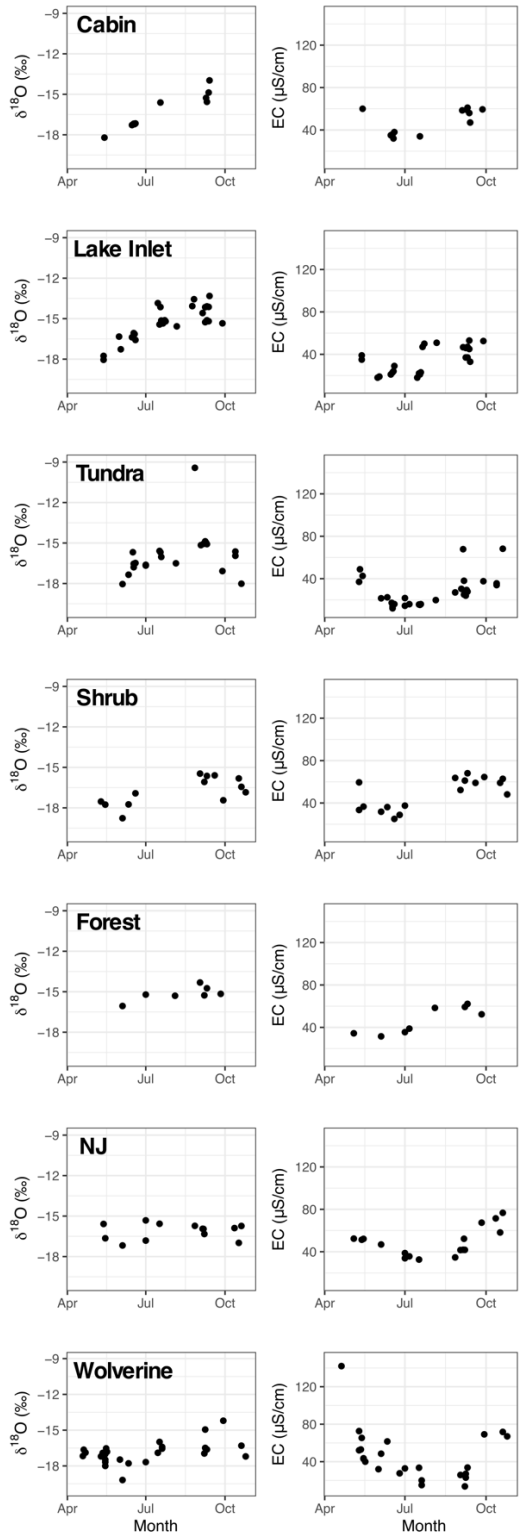

Figure 2.5. Timeseries of $\delta^{18}O$ and EC data collected between 2016-2022. Plots are displayed by location and compile all year's data.

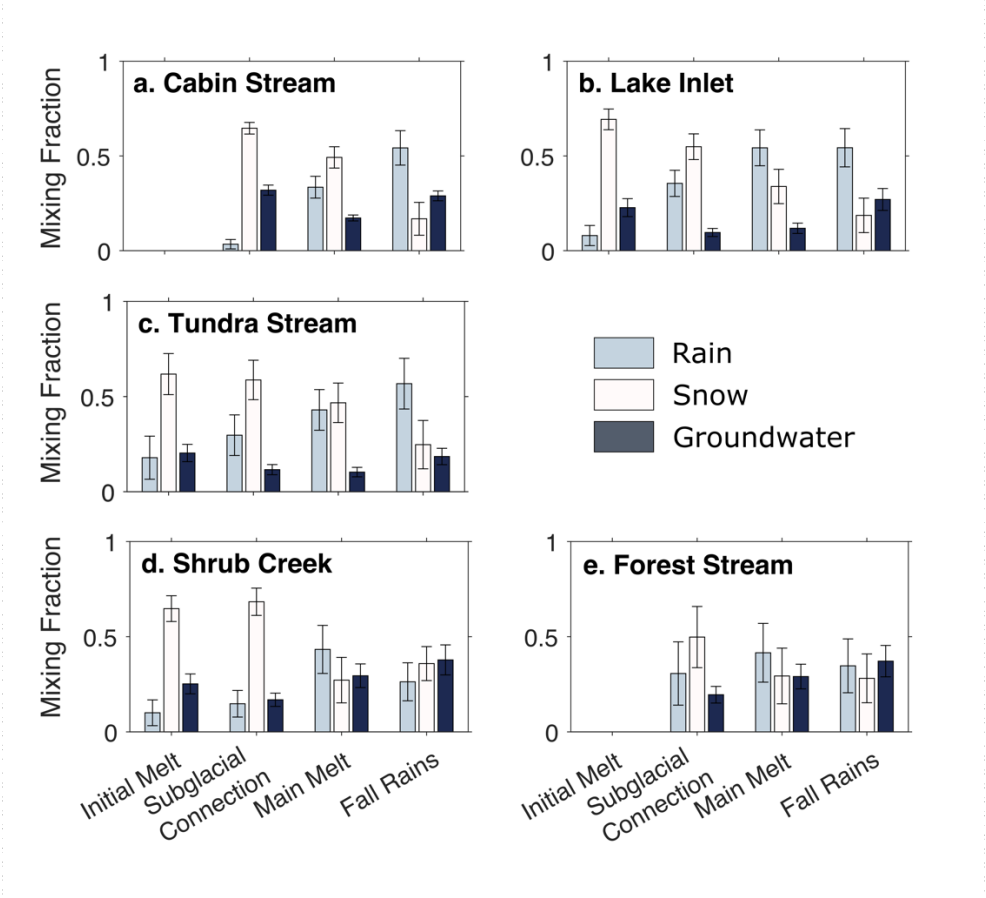

Figure 2.6. Proportions of source waters contributing to non-glacier stream flow in a) Cabin Stream, b) Lake Inlet, c) Tundra Stream, d) Shrub Creek, and e) Forest Stream. Cabin Stream has the highest mean elevation and Forest Stream has the lowest.

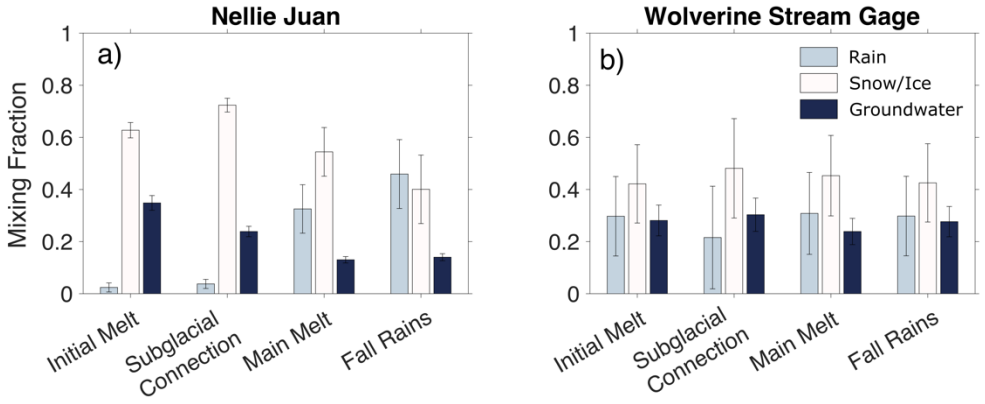

Figure 2.7. Proportions of source water contributions in glacierized streams. The entire Nellie Juan basin is shown on the left, while the Wolverine Glacier basin is shown on the right.

3.4 Glacierized vs. Non-glacierized Streams

Streams with glacial input to streamflow show different patterns in source water contributions than non-glacial streams. In both glacial streams sampled, the snow and ice contribution peaks later than the non-glacial streams (Figure 2.7). Contributions of snow/ice are highest in P2 rather than P1 in glacial streams. The smaller and more glaciated Wolverine basin has less pronounced seasonal trends in source water contribution than the larger and less glaciated Nellie Juan basin. Snow- and ice-melt is the primary contributor to streamflow in all four periods in the Wolverine basin, although the magnitude is only about 10-20% greater than other sources. Snow and ice contribution conversely tapers off in the Nellie Juan basin between P2-P4 and is replaced by rain as the primary contributor by the fourth period.

Table 2.3 The mean elevation and area of each sub-watershed assessed in the mixing model and land cover classification.

	Forest	Shrub	Lake Inlet	Tundra	Nellie Juan	Wolverine	Cabin
Mean Elevation (m)	86	766	820	903	1117	1165	1206
Area (km^2)	0.9	2.5	0.07	2.5	313	24.3	0.5

4. Discussion

As glaciers continue to thin and retreat, landscapes previously covered by ice will transition to deglaciated mountain landscapes. Glacially influenced streams exhibit different source water contributions compared to neighboring off-glacier streams, meaning that changing glacier cover will impact stream hydrology physically and biogeochemically (Figures 2.5 and 2.7). Previous mountain hydrology research has been

focused on regions like the Alps, Andes, and the Rockies (Andermann et al., 2012; Wilson et al., 2004; Baraer et al., 2009; Carroll et al., 2018; Clow et al., 2003; Foks et al., 2018, and others), with very few studies considering non-glacierized catchments in Alaska. This study fills a gap by explicitly examining the source waters driving non-glacier streamflow while simultaneously comparing non-glacial to glacial sub-watersheds that experience similar precipitation regimes and temperatures.

4.1 Source Water Contributions Vary as Percent Glacier and Elevation Changes

Our analysis compared basins of varying percent glacier cover and size and found that the timing and relative proportion of source waters varies between glacierized catchments. The Nellie Juan basin (450 km^2 and ~30% glacierized) had more defined seasonal trends than the Wolverine basin (24.6 km^2 and ~60% glacierized) (Figure 2.7). The larger Nellie Juan basin is dominated by snow and ice melt in periods 1 through 3. Rain inputs in the Nellie Juan basin increase throughout the season as groundwater decreases. By contrast, the source water partitioning in the Wolverine basin appears fairly static across all four periods. The error associated with the Wolverine basin results should be taken into consideration, as the ranges exhibited by the error bars in Figure 2.7 indicate a significant amount of uncertainty. The error may be explained by spikes in EC measured in the early summer as subglacial networks connect (Bergstrom et al., 2021; Figure 2.4). The range of EC values is confirmed in continuous EC data measured at the USGS gauge co-located with the sample site (Figure 2.2). The grab sample data may not accurately capture the range of processes that contribute to streamflow. I expected to see a less seasonally driven result at Nellie Juan because the EC and $\delta^{18}O$ values observed are far less dynamic than those at Wolverine (Figure 2.4). Muted seasonal trends in the Nellie

Juan basin may be attributed to the larger size of the watershed (Table 2.3), contributing to a broader range of travel times and obscuring seasonal source signatures (McGuire and McDonnell, 2006).

Our mixing model results indicate that glacierized streams peak in relative snow/ice contribution later in the year when compared to non-glacierized streams, which is a phenomenon that has been well-documented in glacierized basins (Fountain and Tangborn, 1985). In non-glacial streams, snow contribution is directly linked to the amount of snow melting on the landscape, which tends to increase during spring melt and decline as the season progresses. Glacierized basins experience an initial pulse of snowmelt in streamflow, but transition to a period of ice melt when temperatures reach their maximum and snow has melted from the surrounding landscapes (Fountain and Tangborn, 1985; Hock et al., 2005; Curran and Biles, 2021). The peaking of ice/snow contribution observed in P2 of our glacierized stream mixing model is likely capturing ice melt that is not present in the non-glacial streams in the same region.

Differentiating between snow and ice melt in streamflow using chemical tracers is difficult (Chiogna et al., 2014; Blaen et al., 2014; Vaughn and Fountain, 2005). Isotopic signatures in snowmelt and ice melt both vary seasonally, and their isotopic signatures tend to overlap, as was the case with our samples (Table 2.2, Chiogna et al., 2014). The quantification of contributions of glacier melt versus snowmelt is equally challenging using a physically based modeling approach, given that the volume of snow and ice melt is unknown (Armstrong et al., 2019). The inability to adequately separate snowmelt and ice melt in downstream hydrology is a current limitation in examining the complexities of the dynamics of melt timing.

I compared off-glacier streams across an elevational gradient and found that source water contributions reflected changes in precipitation type and groundwater input. When viewed using a space-for-time approach, high elevation streams represent colder, more snow-dominated basins while low elevation streams represent warmer, more rain- and groundwater-dominated basins. As snowmelt contributes less to streamflow, spring and fall rains may become the main drivers of peak streamflow resulting in flashier flows and warmer stream temperatures (Curran and Biles, 2021).

4.2 Groundwater May Become an Increasingly Important Driver of Streamflow as Temperatures Warm

Groundwater plays an important role in buffering streamflow by storing meltwater and releasing it over long periods of time (Foks et al., 2018; Somers et al., 2019; Baraer et al., 2015). Streams with high groundwater inputs are more resilient to climate extremes and provide steady inputs to flow regardless of precipitation (Hayashi, 2020; Taylor et al., 2013; Carroll et al., 2018). The relative contribution of groundwater increases as the percent glacierized area decreases, indicating that groundwater will become increasingly important for streamflow generation as catchments transition from glacierized to non-glacierized (Baraer et al., 2015). Our results indicate that groundwater contribution is highest in the fall and at low-elevation sites, suggesting that groundwater will become an increasingly important driver of streamflow as summers become drier, fall rains become flashier, and glacier melt contributes less to streamflow (Barnett et al., 2005; Musselman et al., 2017).

High-relief watersheds generate deep flow paths that resurface groundwater in streams at lower elevations (Forster and Smith, 1988; Toth, 1963). The highest elevation

site, Cabin Stream, interestingly had higher proportions of groundwater than other sites representing snowmelt-dominated streams. Increased groundwater contributions may be explained by the topography of the contributing area of the sub-watershed, in which the stream flows through a fairly flat meadow parallel to the base of a steep contributing slope. The change in slope may create localized flow paths of groundwater that resurfaces in streamflow (Forster and Smith, 1988).

Groundwater will likely provide consistent streamflow at shorter timescales, but the impact of warming temperatures on groundwater recharge is unknown (Somers et al., 2019). Snowmelt is a significant contributor to groundwater recharge in snowmelt-dominated basins (Carroll et al., 2018). Glaciers have been shown to contribute very little to groundwater based on physical and hydrochemical studies, meaning that the rate of glacier melt will not likely affect recharge rates (Figure 2.8; Somers et al., 2019; Baraer et al., 2015). The mechanisms for low glacier groundwater recharge are unclear and likely vary depending on local bedrock lithology, precipitation, and topography (Somers et al., 2019; Markovich et al., 2016; Tague et al., 2008). Recharge patterns will likely be affected by changing precipitation regimes, storm intensity, and snowmelt timing, but the exact ways in which these dynamics interact to impact recharge rates are unknown (Musselman et al., 2017; Somers et al., 2019). Groundwater movement and storage capacity are also unresolved, as flow paths in the study region and the depth to unfractured bedrock are unknown (Figure 2.8).

This study uses the signature of what is inferred to be deep groundwater as an end member in the mixing model. Groundwater has many flow paths and residence times and would ideally be separated into shallow and deep groundwater (Forster and Smith, 1988;

Toth, 1963). In mountain systems, shallow groundwater often plays a significant role in streamflow generation (Denning, 1991; Kampf et al., 2015; Foks et al., 2018). I attempted to separate shallow vs deep groundwater using dissolved organic carbon, which is a commonly used tracer due to the higher levels of carbon present in soils (Baron & Mast, 1992). Our results were counter to expectations, and we were unable to find a suitable tracer to separate shallow from deep groundwater and therefore shallow groundwater is omitted.

Although I refer to groundwater as shallow or deep, I consider shallow and deep groundwater to be two ends of a spectrum rather than two separate end members. For example, chemical attributes like specific conductivity are a function of subsurface residence time, resulting in a range of values rather than two clusters (Figure 2.8). The mixing space shown in Figure 2.4 illustrates the concept of shallow groundwater existing as a gradient between stream samples and deep groundwater. Shallow groundwater certainly contributes to streamflow and without shallow groundwater integrated into the model, each of the current three end-members may be overestimated.

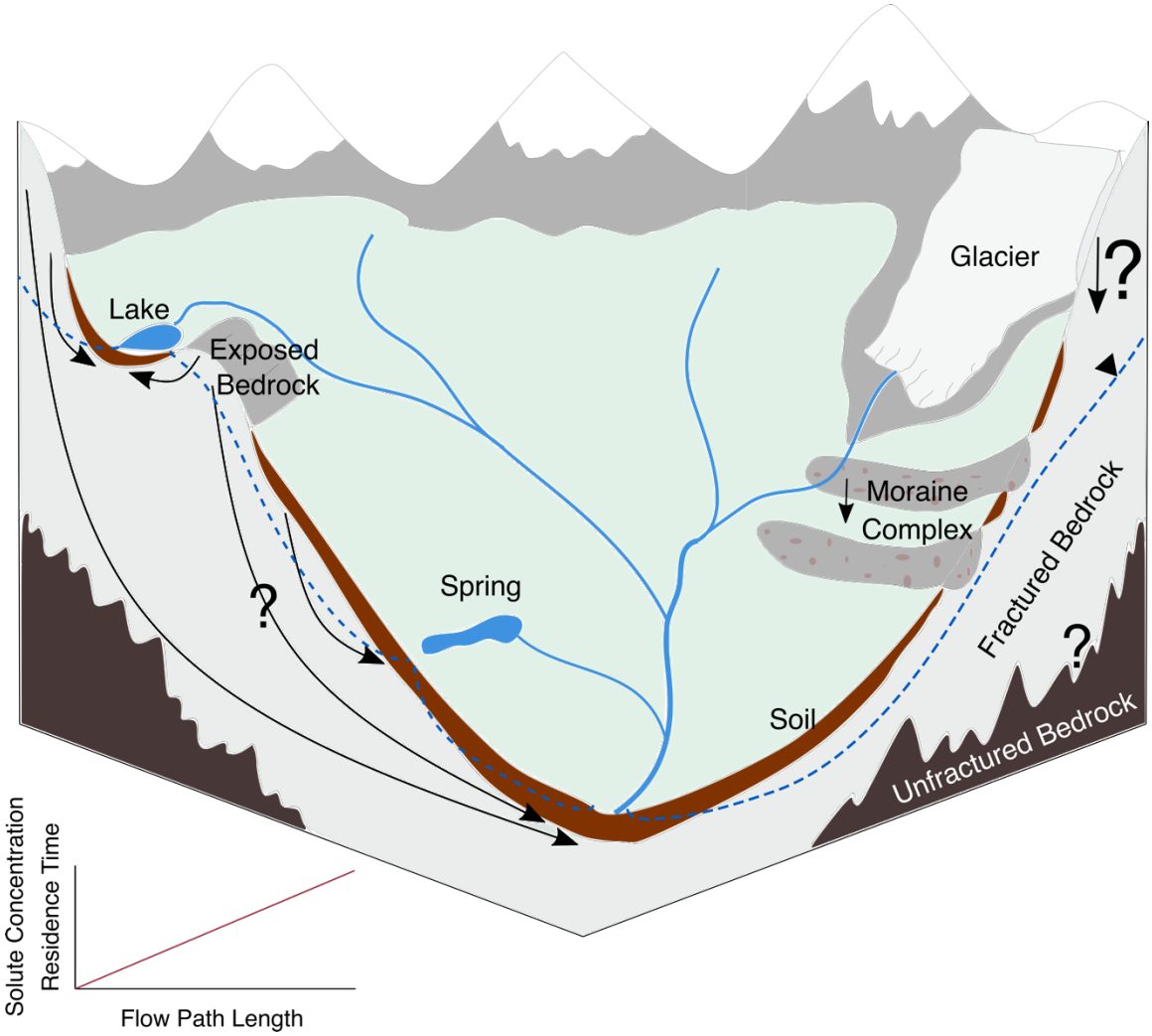

Figure 2.8. Conceptual diagram of groundwater flow paths in a partially glaciated basin. Shallow and deep water are considered to be a continuum rather than two end members, as demonstrated by a range of flow paths.

4.3 Implications of Changing Source Waters

Source water contributions will change in the face of a warming climate, which will shift the timing and magnitude of streamflow as well as chemical and nutrient fluxes (Stephenson, 1990; Eagleson, 1978; Budyko et al., 1974; Holdridge, 1967). When using a space-for-time approach to approximate climate change, our mixing model results offer scenarios ranging from rain-dominated forested systems to snow-dominated alpine tundra streams.

To further contextualize sub-watersheds, I performed a supervised classification of land cover (Appendix A) providing a snapshot of vegetation across the Nellie Juan basin. Warming temperatures support the growth of woody vegetation, and like precipitation, changes occur over elevational gradients. The type of vegetation present on the landscape impacts soil development, nutrient availability, and water demand (Tedrow and Harries, 1960; Klaar et al., 2015; Eagleson, 1978).

Shrubification, or the densification and encroachment of shrubs, is happening rapidly in deglaciating landscapes and may impact source water contributions. Shrubs currently occupy the space between alpine tundra and forest, while also colonizing surfaces exposed by glacial ice within a century of exposure (Figure A.1). The density and extent of shrubs will increase and impact the partitioning of waters. Shrubs will increase transpiration demand, although the way in which shrubs will affect the proportion of source waters contributing to streamflow is unknown. Although groundwater stores seem like promising buffers in the face of droughts (Foks et al., 2018), the benefits may be temporary as recharge decreases and ET increases (Somers et al., 2019). Shrubs will additionally impact snowfall distribution and melt patterns (Sturm et al., 2001), which will in turn impact the proportion and timing of snowmelt in streamflow. Vegetation cover and change should be integrated into predictive studies because they will change the way water is stored, transported, and used in a basin.

As source waters change, streams will shift physically and biogeochemically. Glaciers host microbial communities that serve as a source of bioavailable carbon for downstream ecosystems (Hood and Berner, 2009). Glacial meltwater also provides weathering-derived nutrients like phosphorus and iron to nearshore environments and

high suspended sediment loads (Hood and Scott, 2008; Hallet et al., 1996). Streams draining vegetated non-glacial basins export high concentrations of soil-derived nitrogen and plant-derived carbon (Hood and Scott, 2008). Suspended sediment load and fluxes of labile carbon, phosphorus, and iron will decrease as glacial meltwater contributions diminish. Nitrogen and carbon fluxes will increase as vegetation distribution and density increases. Ecosystems are changing in response to decreases in glacial meltwater, increasing macroinvertebrate biodiversity (Milner et al., 2009).

5. Conclusion

Landscapes are becoming deglaciated, precipitation is shifting to be more rain-dominated, and vegetation is increasing in response to warming temperatures. The hydrology of glacierized and non-glacial basins are well studied, but the transition of this process is poorly understood from a hydrologic perspective and is particularly understudied in Alaska (Curran and Biles, 2021). This research fills a gap by using a space-for-time approach across a range of glacierized and off-glacier basins. I quantified source water contributions across basins using a three end-member mixing model and compared the ways in which precipitation type and percent glacier cover impact stream contribution and timing. I found that glacier melt contributes to streamflow later in the season than snowmelt and glacierized streams exhibit a higher proportion of snow/ice contribution during peak glacier melt. High-elevation watersheds are more driven by snowmelt, while low-elevation basins are more driven by groundwater. Groundwater proportions were highest at low elevations and during the initial snowmelt and fall rain periods.

As temperatures continue to increase, the region will likely trend towards a more rain-dominated system with more vegetation, ultimately impacting source waters. Our findings suggest that streamflow may become increasingly reliant on groundwater as snowmelt and glacier melt decrease. This study demonstrates that source waters vary along elevational gradients and between glacierized and non-glacier streams, which ultimately impact the timing, magnitude, and quality of water downstream.

CHAPTER THREE: DRIVERS AND SCALES OF CHEMICAL WEATHERING IN A TEMPERATE GLACIERIZED BASIN

1. Introduction

Temperate glacierized basins are some of the most physically erosive environments on Earth (Anderson, 2005; Hallet et al., 1996). Glaciation drives the development of erosional features and the redistribution of eroded sediment, which produces a large proportion of highly reactive fresh facies (Anderson, 2005; Tranter, 1982; Wadham et al., 2001). Silt-sized particles are particularly reactive due to the high surface area available for weathering, and glacial till contains large proportions of silt-sized particles (Anderson, 2005; Stumm and Morgan, 2012; Hallet et al., 1996). High rates of glacial physical erosion alter the chemical constituents of streams by supplying highly weatherable material (Anderson et al., 1997).

Chemical weathering can occur in both carbonate and silicate rocks. Carbonates weather on much shorter timescales than silicates and have been shown to be the dominant weathering process in proglacial streams regardless of bedrock type (Deuerling et al., 2019; Torres et al., 2017; Raiswell, 1984). Silicate weathering occurs over longer time scales and is positively correlated with runoff magnitude. Silicate weathering can therefore still make significant flux contributions of silicate-derived ions due to the high flows observed in glacial streams (Anderson, 2005).

Water moving through fresh facies will have higher proportions of ions derived from carbonates (i.e. HCO_3^-, Ca, and Mg), and water moving through older facies will

have higher proportions of ions derived from silicates (i.e. SiO_2) due to the preferential weathering of carbonates (Jenckes et al., 2022; Wimpenny et al., 2011). Factors that control weathering (i.e. bedrock type, temperature, and discharge) can vary greatly, complicating the relationship between carbonate and silicate weathering. The type of weathering can be determined using known ionic ratios, which can aid in the understanding of how weathering patterns change across a range of glacially influenced streams.

Glacially-derived weathering can majorly influence chemical weathering fluxes and atmospheric CO_2 concentrations at a global scale (Gibbs and Kump, 1994; Tranter et al., 2003; Eiriksdottir et al., 2013). For example, silicate weathering by carbonation produces alkalinity, which aids in the removal of atmospheric CO_2 (Berner, 2004). Carbonate weathering by sulfide oxidation, however, supplies CO_2 to the atmosphere (Torres et al., 2017; Liu et al., 2011; Ryu and Jacobson, 2012). The net influence of carbonate and silicate weathering is still poorly understood, and it is unknown if glacial weathering serves as a carbon source or sink.

Previous studies have examined weathering regimes and stream chemistry changes along proglacial streams on the order of kilometers (Anderson et al., 2000; Deuerling et al., 2019), but no studies have examined glacial weathering patterns on finer scales or compared proglacial streams to adjacent off-glacier streams. In this research, I aim to answer the question: What are the major drivers of weathering-derived solutes in glacierized basins? I hypothesize that glacially influenced streams will have higher carbonate weathering rates than non-glacial streams, while non-glacial streams will have higher silicate weathering rates. I additionally hypothesize that non-glacial streams that

pass over glacial trimlines from the LIA (~1300 to 1850 CE) will have increased concentrations of weathering-derived solutes due to the presence of more recently exposed weatherable rock. To answer this question, I compare solute concentrations in glacierized and non-glacial streams to determine the role of modern-day glaciation in weathering. I additionally compare ion, nutrient, and isotopic values in non-glacial streams above and below glacial trimlines from the LIA to examine the influence of recent glaciation. Finally, I use a three end-member mixing model to compare stream source water contributions and examine the relationship between groundwater contribution and weathering-derived solutes. This research has implications for the spatial and temporal scales at which chemical weathering occurs, what factors drive chemical weathering, and how glaciers influence global carbon cycling.

2. Methods

2.1 Study Site

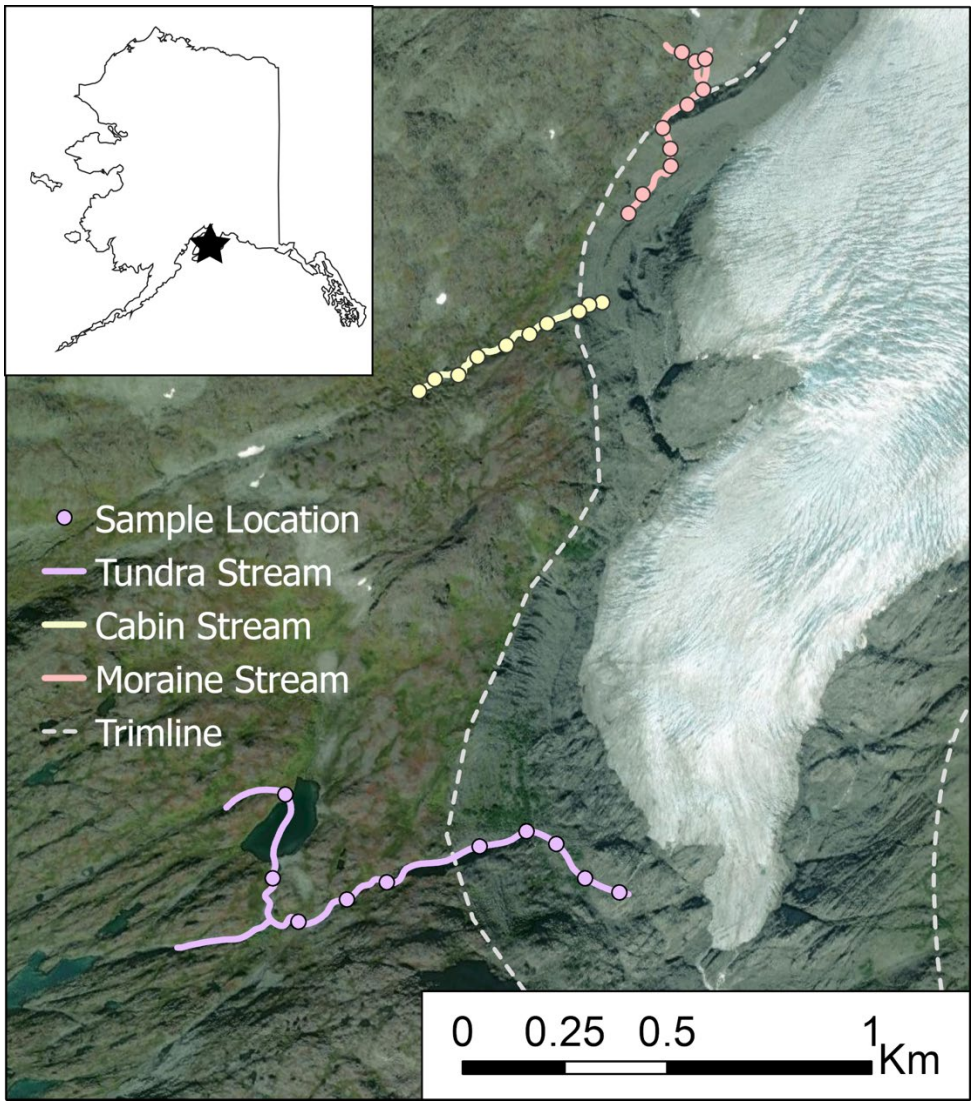

Figure 3.1. Site map of sampling region. Inset map shows the location in reference to the state of Alaska. Streams are outlined by color and sampling points are marked with a circle of the corresponding stream color. The glacial trimline left behind by the LIA is outlined by the grey dashed line surrounding the Wolverine Glacier.

This research takes place within the Wolverine Glacier watershed, located in south-central Alaska on the Kenai Peninsula. The Wolverine Glacier watershed is 24.6

km^2 and ranges from 360 to 1680 m in elevation. Mass balance and streamflow measurements have been made by the USGS since 1966. The Wolverine Glacier covers ~60% of the basin. In addition to monitoring mass balance and discharge, the USGS has operated a meteorological station located at 990 m adjacent to the glacier since 1968. The Wolverine Glacier watershed is drained by Wolverine Creek, which flows into the Nellie Juan River. The Nellie Juan River terminates at Kings Bay, a part of Prince William Sound. The region is characterized by a maritime climate. High elevations are characterized by rock, alpine tundra vegetation, and snow that persists in patches throughout much of the summer. Soils in areas covered by tundra vegetation are likely Cryod-Cryorthent type, are shallow, acidic, rich in rock fragments, and well drained (van Patten, 2000). The bedrock in the region is metasedimentary, including greywacke, siltstone, and shale (Wilson and Hults, 2012).

I sampled three streams in the Wolverine Glacier watershed, ranging in elevation from 600-1200 m. Ten sites were assigned to each stream, spanning the length of each stream (Figure 3.1). The highest-elevation Moraine Stream flows through a sparsely vegetated landscape, crosses over a moraine, and eventually disappears in coarse moraine sediment before reaching the glacier. The Cabin Stream flows through tundra vegetation and eventually transitions into a braided stream that also terminates in coarse moraine sediment. The lowest elevation Tundra Stream drains mixed tundra, shrub, and exposed bedrock terrain. Two alpine lakes, approximately 0.02 km^2 and 0.03 km^2, drain into Tundra Stream before it follows a narrow canyon and disperses into a braided stream that eventually reaches the glacier. Each of these streams crosses a trimline left by glaciation during the LIA (~1300 to 1850 CE), an erosional feature marking the maximum vertical

extent of the glacier (Figure 3.1). Moraine, Cabin, and Tundra Streams were sampled over reaches that were 500, 500, and 1250 m respectively. All but one sample was taken below the lakes on Tundra Stream (Figure 3.1).

Table 3.1 Sample stream physical characteristics. Mean elevation and slope values are of the sample reach.

	Moraine	Cabin	Tundra
Mean Elevation (m)	955	957	725
Sample Reach Length (m)	370	400	1200
Mean slope (°)	24	14	11

2.2 Field Data Collection

Tundra, Cabin, and Moraine streams were sampled synoptically in early August and early September of 2022. Stream samples intended for nutrient and ion analysis were filtered in the field using a syringe and a 0.45μm Millipore filter. Nutrient and ion samples were collected in 60 mL HDPE bottles that had been pre-cleaned by soaking and triple rinsing with DI and triple rinsed with filtered sample water. They were then stored at -20°C upon returning from the field until analysis. Isotope stream samples were collected unfiltered in 30 mL HDPE bottles and filled to the top to minimize head space. Isotope samples were stored at +4°C. In the field, all samples were stored in coolers to prevent unwanted warming or freezing. Electrical conductivity (EC) and temperature data were collected using a YSI Ecosense 300 handheld probe (accuracy ±1% of reading). For water temperatures above 1.7°C, the probe automatically compensates EC to 25°C. Below 1.7°C, the following equation was used to compensate stream EC to 25°C.

$$EC_{Corrected} = \frac{EC_{Uncorrected}}{1+(0.0191*(T-25)} \quad (3.1)$$

I used additional data from the region to compare glacierized to non-glacial streams and to define source water end-member signatures. These data span six years of sampling campaigns and are sourced from Koch et al. (2021), which will be appended and republished with more recently collected samples. Sample collection and processing methods for these data are described in Bergstrom et al. (2021) and Chapter 2 of this thesis.

2.3 Laboratory Analysis

Ions and nutrients were measured on a Metrohm 930 Compact IC Flex ion chromatography system and a SEAL Analytical AA500 segmented flow nutrient analyzer (accuracy <± 0.004 mg/L for ions, <±0.004 mg/L for NO_x, and <±0.30 for SiO_2). Calibration curves were developed to span the observed range of concentrations and detection limits were calculated using equation 3.2:

$$Detection\ Limit = \frac{3.3*\sigma}{m} \quad (3.2)$$

Where σ is the standard deviation of the residuals and m is the slope of the calibration curve. Detection limits were applied to ensure statistically significant results in the low-level range (see Table 3.2).

Table 3.2 Detection limits of nutrients and ions.

Ion/Nutrient	NO_X	SiO_2	Na	NH_4	K	Mg	Ca	F	Cl	NO_2	NO_3	PO_4	SO_4
DL (mg/L)	0.001	0.0015	0.003	0.003	0.008	0.002	0.003	0.003	0.005	0.003	0.002	0.002	0.007

I conducted isotope analysis using a Los Gatos Research Liquid-Water Isotope Analyzer (LWIA) at Boise State University (accuracy <± 0.12‰ for $\delta^{18}O$ and <±1.1‰ for $\delta^{2}H$, precision <± 0.25‰ for $\delta^{18}O$ and <±1.90‰ for $\delta^{2}H$). The range of standard waters spanned -6.62‰ to -37.5‰ $\delta^{18}O$ and -41.6‰ to -302.0‰ $\delta^{2}H$.

2.4 Sea-salt Corrections

Due to the proximity of the sample site to the ocean, I observed an excess of sea-salt derived ions in stream samples. To account for marine-derived ions, I corrected stream samples using known sea-salt ratios using equation 3.3:

$$[Non\ Sea - salt]_{ion} = [ion] - (SSratio\ \times\ [Cl]) \tag{3.3}$$

where ions K, Na, Mg, SO_4, and Ca were corrected using Cl.

2.5 Calculation of Bicarbonate

Bicarbonate was calculated using the charge balance method, in which the concentrations of ions were converted to meq/L and the following equation was used:

$$\sum cations - \sum anions = [HCO_3^-] \tag{3.4}$$

assuming that the difference in charge is explained by bicarbonate. This method is dependent on samples being within the pH range that bicarbonate species can exist in.

2.6 Mixing Model

To assess the proportion of stream source waters in each stream, I used a three-component end-member mixing model. End members were identified as snow, rain, and deep groundwater. Sample data used in this study (end members and stream samples from nearby sites) are sourced from (Koch et al., 2021), which will be appended and republished with more recently collected samples. Sample collection and processing methods for these data are described in Bergstrom et al. (2021) and Chapter 2 of this

thesis. Our dataset did not have a suitable tracer to distinguish between deep and shallow groundwater, and thus only deep groundwater is considered in the model. The model used EC as a tracer to distinguish meteoric from groundwater, and $\delta^{18}O$ to distinguish rain from snow. The model is expressed as follows:

$$1 = f_{rain} + f_{snow/ice} + f_{gw} \tag{3.6}$$

$$C_{stream} = C_{rain}f_{rain} + C_{snow/ice}f_{snow/ice} + C_{gw}f_{gw} \tag{3.7}$$

where C represents the value of each tracer and *f* denotes the fraction of source water present in the stream. When calculating mixing fractions for each stream, the average value of tracers EC and $\delta^{18}O$ were used. For example, all EC measurements taken in the Cabin Stream in August of 2022 were averaged and that value was used in the model. Generally, there were 10 samples collected along each stream each day. A Monte Carlo simulation was used due to the high variability in measured end-member values and the low number of samples. End member values were randomly sampled within one standard deviation of the mean in each iteration of the model. If stream samples fell within the mixing space created by end member values, the proportion of each stream source value was retained. This iteration occurred 10,000 times, and the mean of all retained values is displayed in the final model.

3. Results

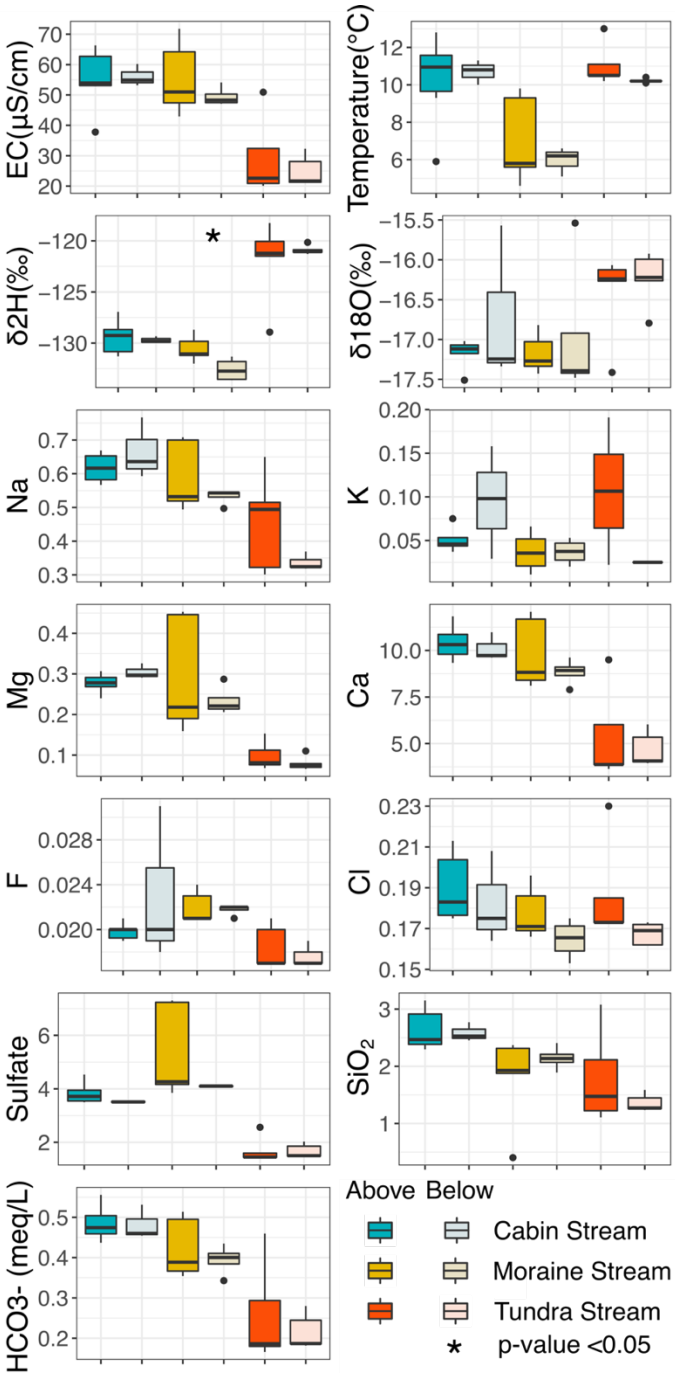

Figure 3.2. Box plots display the range of values measured above and below the LIA trimline in three streams in early August, 2021. Cabin Stream is displayed in blue, Moraine in yellow, and Tundra in red. Darker hues indicate samples taken above the trimline and lighter hues indicate samples below the trimline.

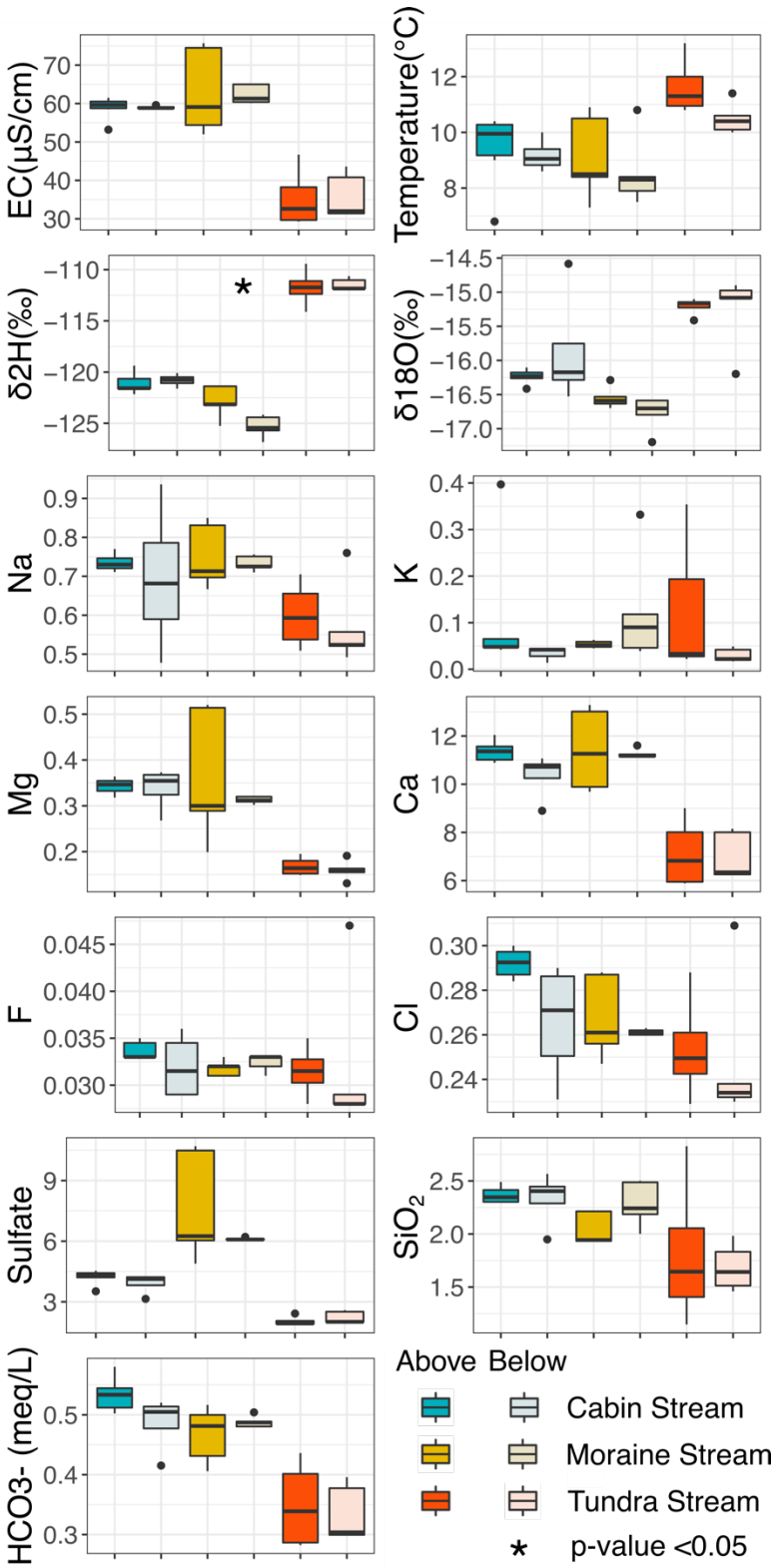

Figure 3.3. Box plots display the range of values measured above and below the LIA trimline in three streams in early September, 2021. Cabin Stream is displayed in blue, Moraine in yellow, and Tundra in red. Darker hues indicate samples taken above the trimline and lighter hues indicate samples below the trimline.

3.1 Stream Chemistry Above and Below Trimlines

In most cases, there are no significant differences in stream water chemistry above and below trimlines (Figures 3.2 and 3.3). Mean nutrient and ion concentrations are often higher above the trimline than below, although this is not true for all cases. Temperature, isotope values, and EC do not change significantly above and below trimlines.

Stream chemistry exhibits a change between early August and early September sampling (Figures 3.2 and 3.3). In September, ion, nutrient, bicarbonate, and EC values are higher than in August. Isotopes are more enriched in September. Silica was the only constituent that did not show a change in concentration between August and September.

Tundra Stream has lower Ca, Mg, and SiO_2 concentrations than Moraine and Cabin streams in both months (Figures 3.2 and 3.3). Moraine and Cabin streams have lighter isotope signatures and higher EC values than Tundra Stream. In August, Moraine Stream is colder than Cabin and Tundra streams, although this trend is not observed in September (Figures 3.2 and 3.3).

3.2 Weathering Chemistry

Prior to analyzing data for weathering patterns, a sea salt correction was made due to the proximity of the ocean and elevated ion concentrations in rain samples. All stream sample ion concentrations were corrected to Chloride because very few samples had excess Chloride concentrations beyond known sea-salt ratios (Figure 3.4). Sodium and Magnesium were also considered, but samples fell above known sea salt ratios suggesting other sources of these ions in the watershed (Figure 3.4).

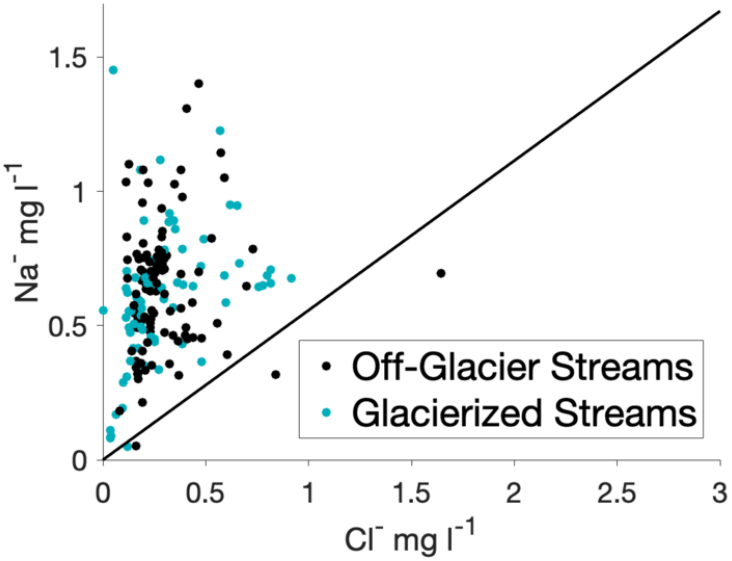

Figure 3.4. The relationship between ion concentrations were plotted for stream samples. Black circles indicate non-glacial streams and blue circles represent glacially influenced streams. The thick black line plots the known ratio between ions in seawater. Cl was chosen as the ion to be corrected to because few samples are further enriched in Cl beyond the known sea water concentration.

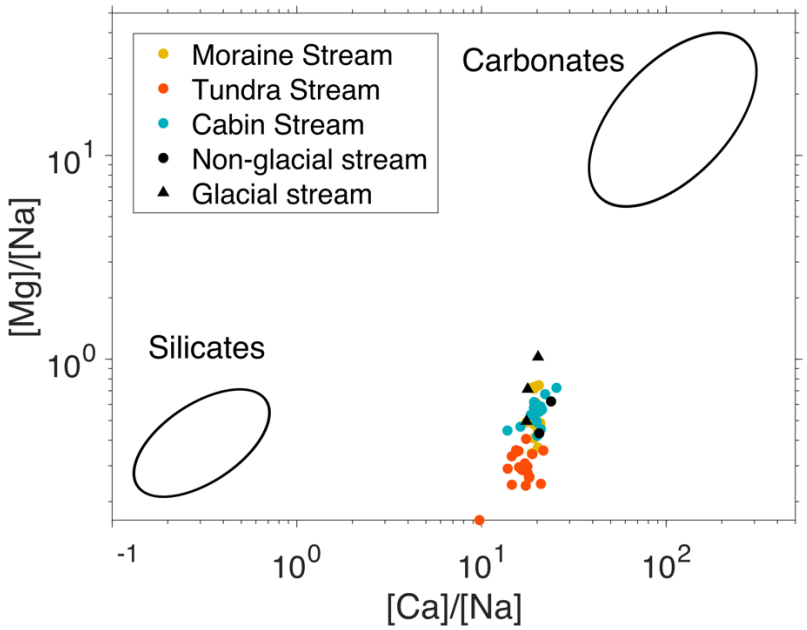

Figure 3.5. The relationship between Mg and Ca normalized by Na in stream samples. Global end members of silicate and carbonate weathering are circled in the corners of the plot. Each sample collected in both August and September field campaigns are plotted, as are the yearly averages for other glacial (triangles) and non-glacial (circles) streams.

Plotting local stream chemistry against end-member ratios of carbonate-dominated and silicate-dominated streams can aid in the understanding of the dominant weathering source of a watershed. Our stream samples plot between carbonate and silicate end-members in the Ca/Na direction, and are nearer to the Mg/Na ratio of silicates (Figure 3.5). Samples from all streams have similar Ca/Na ratios, while Moraine and Cabin Stream samples have slightly elevated Mg/Na ratios when compared to Tundra Stream (Figure 3.5). Other non-glacial streams in the region plot similarly to Cabin, Moraine, and Tundra Streams. Glacial streams show a broader range of Ca/Na ratios when compared to off-glacier streams (Figure 3.6).

The relationship between bicarbonate and silicate can also be used to determine the dominant type of rock being weathered using known stoichiometric ratios (Figure 3.7). Samples that plot below the 2:1 line indicate silicate weathering, while those above the 4:1 line indicate carbonate weathering (Jenckes et al., 2022; Bouchez & Gaillardet, 2014; Ibarra et al., 2016; Maher, 2011; Winnick & Maher, 2018). Our stream samples plot between the 18:1 line and the 4:1 line, indicating carbonates as the dominant weathering source.

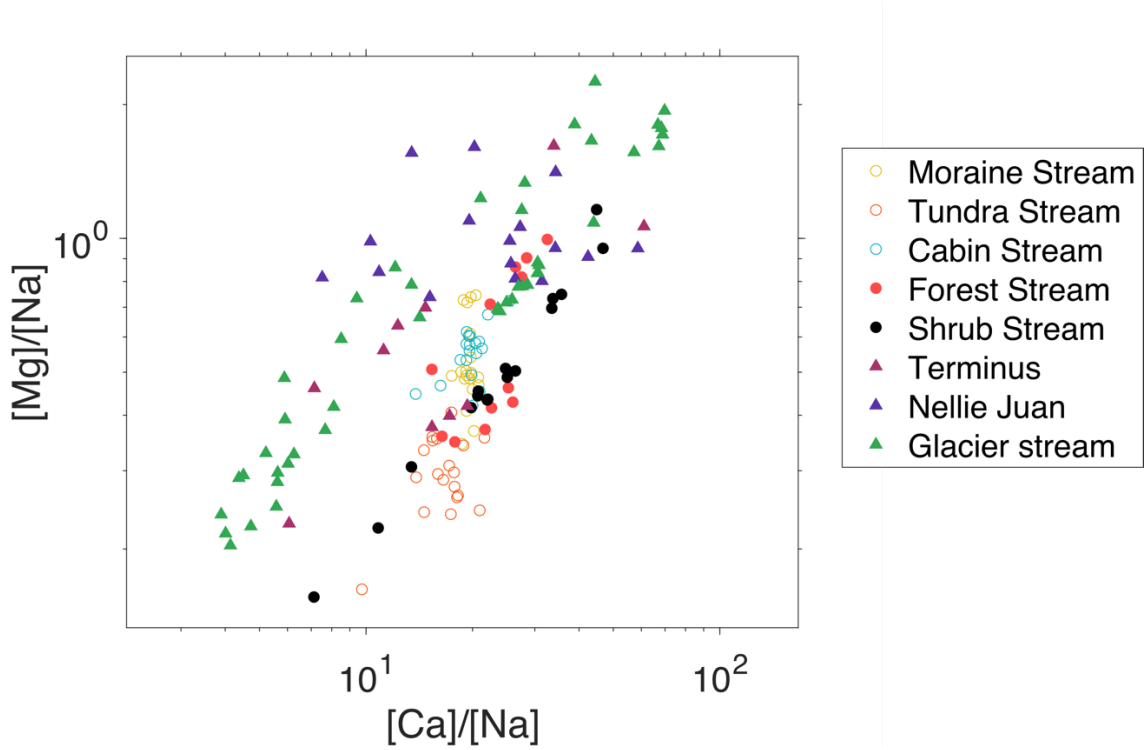

Figure 3.6. The relationship between Mg and Ca normalized by Na for all stream samples. This includes samples taken at all times of year over multiple years. Non-glacial streams are denoted by circles and glacial streams are denoted as triangles.

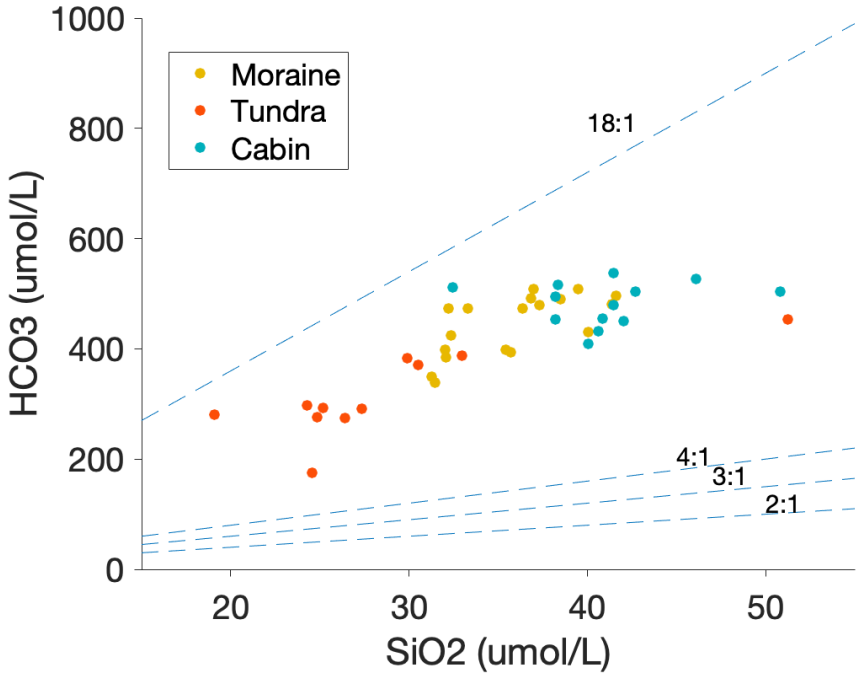

Figure 3.7. Bicarbonate and silicate relationships for stream samples collected in August and September, 2021. Samples above the 4:1 line indicate carbonate weathering and those below the 2:1 line indicate silicate weathering.

3.3 Source Water Change

The mixing model shows distinct changes in source water contributions between sampling campaigns. In early August, all three streams have a higher proportion of snowmelt contributing to streamflow than they do in early September (Figure 3.8). Conversely, rain and groundwater contributions increase between the two months.

Cabin and Moraine Streams have almost identical mixing fractions in both August and September (within 2% and 7% for each fraction in August and September respectively). Tundra has higher fractions of rain (~40% in Tundra Stream and ~20% in Cabin and Moraine Streams), and far less groundwater both months. Snowmelt fractions were similar in all three streams each month (~45% in August and ~35% in September).

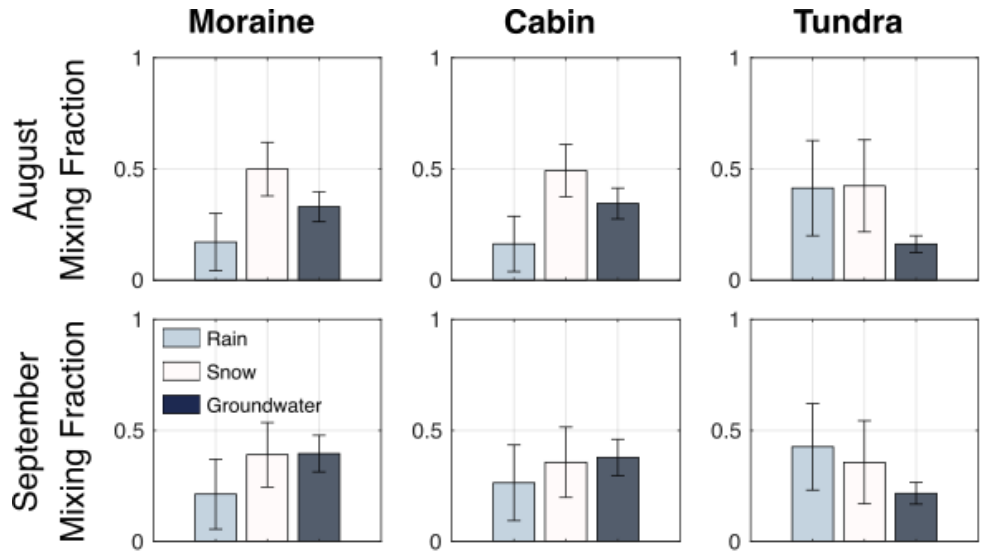

Figure 3.8. Source water fractions generated by a three end-member mixing model. End members rain, snowmelt, and groundwater are light blue, off-white, and dark blue respectively. The model averaged tracer values for all stream samples collected in a single steam on a single day.

4. Discussion

4.1 Limited Differences In Weathering Occurs Below LIA Trimline

The results of stream chemistry changes above and below the LIA trimline indicate that there is no change in weathering patterns as these streams pass over the trimline. I hypothesized that weathering would increase as streams passed through fresh facies, resulting in higher concentrations of ions in the below-trimline samples. Instead, I saw no appreciable difference in ion and nutrient concentrations in relation to the trimline. The lack of measurable weathering changes may be explained by a few factors. First, the short length of streams may result in insufficient time for weathering to occur. The streams flow over bedrock for <.5 km before flowing under the glacier or disappearing into moraine sediments, which is a much shorter distance than other papers that have examined periglacial stream weathering (Deuerling et al., 2019; Anderson et al., 2000). Second, the type of rock (i.e. rock that has been eroded versus deposited) below the trimline may drive weathering potential. Previous studies examined proglacial streams that contained high proportions of silt-sized sediment (Deuerling et al., 2019). This fine-grained sediment can be sourced from subglacial networks that mobilize material eroded by the base of the glacier, and from lateral moraines that streams flow through (Anderson, 2005; Stumm and Morgan, 2012; Hallet et al., 1996). Trimlines, by contrast, are characterized by exposed bedrock and lateral moraines. Higher proportions of exposed bedrock may decrease the presence of silt-sized grains and thus chemically reactive sediment. The exact driver limiting the weathering of short streams over glacial trimlines is unknown and may be explained by a combination of these factors.

Moraine Stream has much higher variability in nutrient/ion concentrations above the trimline than other streams (Figures 3.2 and 3.3), likely because it is downstream of a confluence of two streams draining basins with different topographical attributes (i.e. a steep rocky hillside and a protected bowl with persistent seasonal snow). One sample was taken above the confluence in each of the two streams, while three additional samples were collected between the confluence and the trimline. EC values and ion/ nutrient concentrations were consistently higher in the rocky branch than in the snowy branch.

4.2 Interpretation of Geochemical Weathering Relationships

I examined the concentrations of solutes in streams in two ways to assess weathering. I analyzed the relationship between Mg/Na and Ca/Na (Figures 3.5 and 3.6) and I assessed the relationship between bicarbonate and silicate (Figure 3.7). Each analysis indicates a different primary weathering source.

Carbonate-dominated basins result in higher ratios of weathering-derived Ca/Na and Mg/Na concentrations (Gaillardet et al., 1999). The relationship between Mg/Na and Ca/Na shown in Figures 3.5 and 3.6 implies that both non-glacier and glacierized streams in the region weather a combination of silicates and carbonates. The relationship between bicarbonate and silicate (Figure 3.7) indicates that carbonate weathering is the primary type of weathering in the Wolverine Glacier watershed. Interestingly, no samples lie below the 2:1 line, which would indicate silicate weathering. These results are contradictory to those described in Figures 3.5 and 3.6, which indicate a mix of silicate and carbonate weathering. Bicarbonate was calculated using the charge balance method, which introduces error and may not be as accurate as calculating ion ratios. The presence of error may describe why each analysis indicates different results. However, our results

are consistent with other non-glacierized streams in the region (Jenckes et al., 2022). When combined, these analyses suggest that carbonate weathering is certainly occurring in the region and that silicates may or may not be weathering.

In both analyses, Tundra Stream plots separate from Moraine and Cabin Streams. Tundra Stream has consistently lower Mg/Na ratios when compared to Cabin and Moraine Streams (Figures 3.5, 3.6), and has lower bicarbonate and silicate concentrations (Figure 3.7). Lithology is known to be a major control on weathering products and could explain the differences observed here (Raiswell, 1984; White et al., 2003). The bedrock geology has not been mapped at a fine enough scale to make distinctions between the lithologies of each stream's drainage basin (Wilson and Hults, 2012). However, a topographic step causes an icefall in the Wolverine Glacier at ~860 m and manifests as a steep slope adjacent to the glacier separating the upper two streams from the lower stream. This likely indicates a shift in bedrock type. Geochemical differences observed in streams may therefore be explained by underlying rock and thus differing mineralogy. Additional mapping of the region or geochemical analysis of rocks in each sub-basin would be needed to verify this hypothesis.

Glacial and non-glacial streams occupy similar ranges in Figure 3.5, indicating that the presence of a glacier does not seem to influence the type of weathering occurring. Carbonates weather on a much faster timescale than silicates. A dissolution experiment using glacially derived sediment in the same bedrock unit found that carbonate dissolution only occurred over the timescale of about 900 hours, while silicate weathering increased over much longer timescales (Anderson et al., 2000). I would therefore expect proglacial streams carrying high sediment loads to have greater concentrations of

carbonates than off-glacier streams carrying no freshly comminuted sediment. Instead, our results show that non-glacial streams can weather carbonates at a similar rate to glacial streams (Figures 3.5 and 3.6). The lack of distinction between weathering sources further indicates the importance of bedrock as a driver in weathering-derived solutes.

4.3 Source Water Differences

Snowmelt contribution to streams decreased between August and September, which aligns with snow visible on the landscape between the sampling campaigns (Figure 3.8, Photo 3.1). Rain contribution increased between the sampling periods, which is supported by persistent rain and higher stage values at Tundra Stream through the month of August (Figure 3.9). Groundwater contributions increased between the two sampling periods and can also be explained by high rainfall; saturated soil water likely flushed deeper groundwater into streamflow (Fetter, 2001).

Photo 3.1. Photos taken from the same location one month apart. A snow bridge covers much of the stream in early August, while very little snow remains in early September.

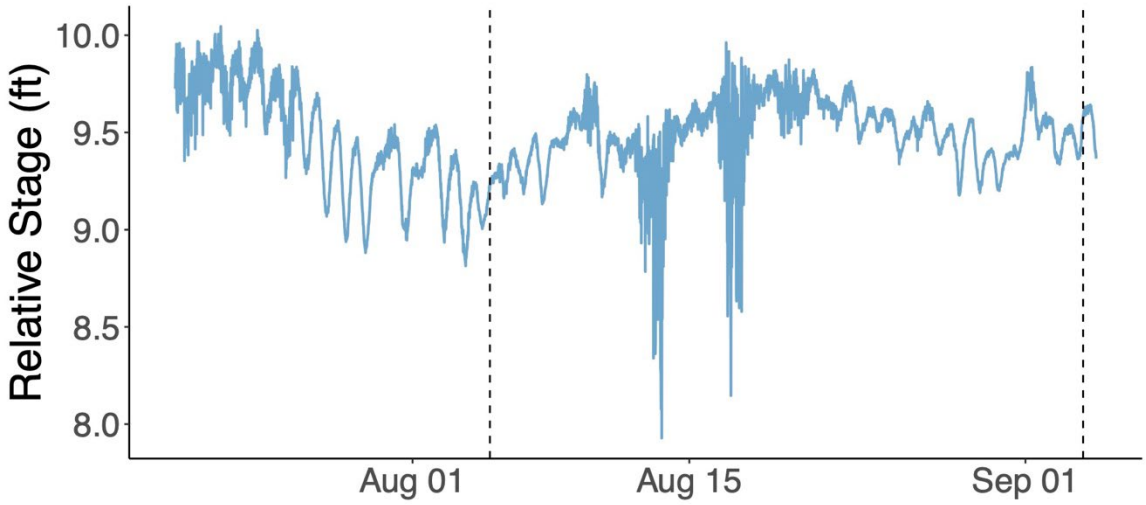

Figure 3.9. Relative stage of Tundra Stream between mid-July and early-September of 2022. Sample collection dates are marked by the vertical dashed lines.

Proportionately, snowmelt consistently contributed less in Tundra Stream compared to Cabin and Moraine streams, while rain contributed more (Figure 3.8). One possible explanation for higher rain proportions could be the enrichment of $\delta^{18}O$ isotopes through evaporative processes in the many lakes that drain into Tundra Stream. Evaporatively enriched $\delta^{18}O$ signatures would cause the model to partition more streamflow to rain since the rain end member is more enriched than snow. To test this theory, $\delta^{18}O$ and $\delta^{2}H$ samples were plotted to create a LMWL for each stream (Figure 3.10). Samples that have been enriched by evaporative processes would plot below the line. Only one such sample was observed, and the possibility that evaporation is causing the model to partition more rain in streamflow is unlikely. The difference may instead be caused by the proportion of snow on the landscape, as Tundra is the lowest in elevation. A considerable number of outliers are observed for each stream in Figure 3.10, which may be explained by the narrow spread of pooling of $\delta^{18}O$ values (~2‰), or evaporative

processes. Outliers were collected in ponded reaches of streams in moraine complexes and in high-snowmelt reaches that have likely undergone fractionation.

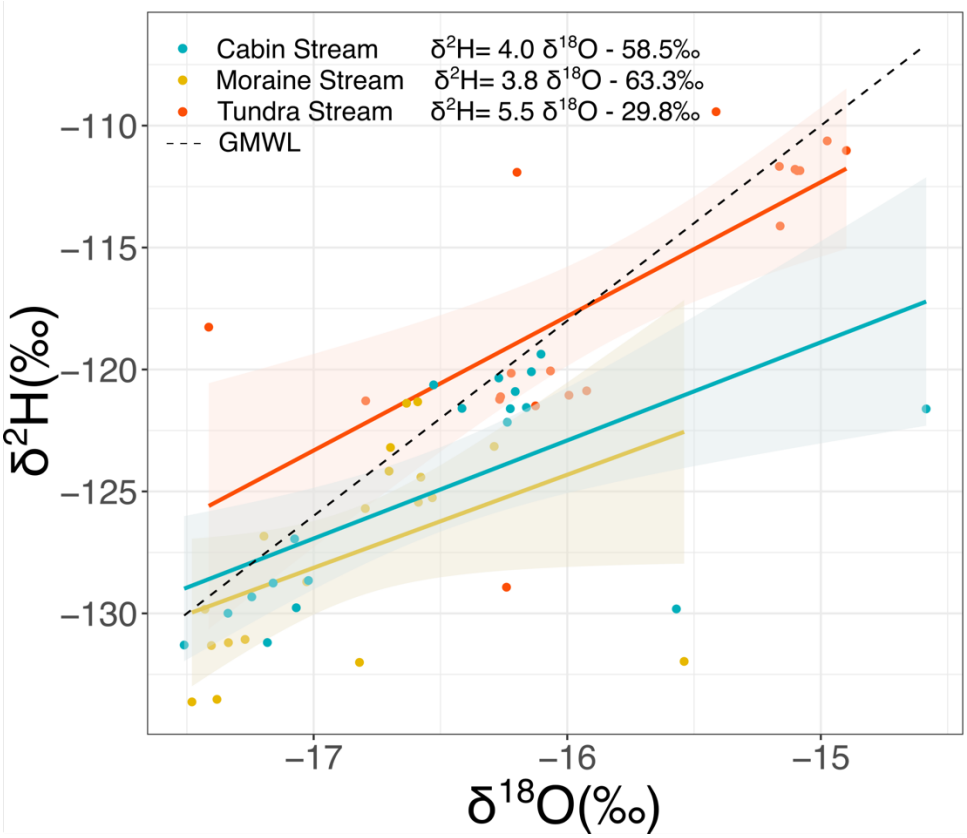

Figure 3.10. LMWL fitted to all samples collected in August and September, 2021 for each stream. The GMWL is plotted in black for comparison.

Notably, Tundra Stream differs from Cabin and Moraine Streams from both a geochemical and source water perspective. Tundra Stream had the highest groundwater proportions and the highest values of bicarbonate, Sulfate, Ca, SiO_2, and Mg:Na ratios (Figures 3.2, 3.3, 3.5, and 3.7). Compared to meteoric water, groundwater has higher concentrations of solutes due to long residence times that promote bedrock weathering. Higher solute concentrations are observed between August and September sampling periods as well; all streams had higher proportions of groundwater (Figure 3.8) and

higher solute concentrations (Figures 3.2 and 3.3). These findings indicate that the concentration of solutes is driven by the proportion of groundwater in streams while ion ratios and relationships are driven by underlying bedrock.

5. Conclusion

I assessed weathering patterns and stream source water contribution in three non-glacial streams adjacent to the Wolverine Glacier in southcentral Alaska. I found that short (<1.5 km) streams do not exhibit a change in weathering patterns below glacial trimlines left behind during the LIA. This may be caused by short timescales in which water could interact with rock or the lack of weatherable silt-sized grains in erosional features such as a trimline. Geochemical analysis suggests that the streams in this region weather both silicates and carbonates. Weathering-derived solutes vary slightly between off-glacier streams, which is likely a function of the underlying bedrock. I additionally found a positive relationship between the concentration of weathering-derived solutes and the proportion of groundwater in streamflow. Glacierized streams in the region had similar weathering-derived solute concentrations to non-glacierized streams, indicating that bedrock rather than glaciers is the driver of solutes in the region.

Future research should be conducted to analyze geochemical differences between the underlying bedrock of each basin to confirm lithology as a driver for differences in stream chemistry. Discharge measurements at each stream would additionally allow for flux measurements, which can give further insight into broader questions regarding the impact of glacial weathering on atmospheric CO_2 sequestration (Gibbs and Kump, 1994; Tranter et al., 2003; Eiriksdottir et al., 2013; Berner, 2004). Our results fill a critical gap by describing a spatial scale at which weathering is limited, showing that small streams

cannot export large quantities of weathering-derived solutes. It additionally assesses non-glacial streams that pass over glacially eroded features from the LIA, rather than examining only proglacial streams. This research supports the body of literature that shows the importance of underlying bedrock mineralogy in stream solute export (Bluth and Kump, 1994).

CHAPTER FOUR: CONCLUSION AND FUTURE DIRECTIONS

The hydrology of glaciated basins is rapidly changing as glaciers thin and retreat, precipitation regimes shift to become more rain-dominated, and vegetation densifies and encroaches on newly exposed surfaces (McAfee et al., 2014; Littell et al., 2018; Adam et al., 2009; Hammond et al., 2019). Source waters are shifting in response to these changes, which affects the physio-chemical properties of streamflow (Milner et al., 2009; Musselman et al., 2017; O'Neel et al., 2014; Hannah et al., 2000). Downstream ecosystems are being affected by these shifts through changes in stream temperature and nutrient and sediment fluxes (Hood and Berner, 2009; Fellman et al., 2015; Milner et al., 2009, 2017). High weathering rates in glacierized basins can impact the global carbon cycle through the production or consumption of CO_2 as a function of the weathering mechanism (Berner, 1995; Torres et al., 2017; Herman et al., 2013; Foster and Vance, 2006; Anderson et al., 2000).

This study examines the potential impacts of warming temperatures on physical hydrology in addition to exploring drivers of weathering patterns in glacierized and deglaciated landscapes. In Chapter 2, I make inferences about changing stream source water contributions using elevation as a proxy for climate change in a space-for-time approach. These findings have implications for downstream ecosystems, as sediment and nutrient fluxes change. In Chapter 3, I examine the drivers of weathering-derived solutes across a similar range of basins. Here, I revisit the major findings of this thesis and discuss possible future directions.

Increasing Temperatures Shift Landscapes and Hydrology

Elevation is a primary control on air temperature, which in turn impacts precipitation regimes, melt timing, vegetation growth, and soil development (Stephenson, 1990; Eagleson, 1978; Budyko et al., 1974; Holdridge, 1967). I use a space-for-time approach to examine off-glacier watersheds across an elevational gradient and make inferences about changing hydrologic regimes in the face of a warming climate. I additionally compare off-glacier watersheds to adjacent glacierized watersheds of varying percent glacier cover and size to contextualize the hydrologic influence of glaciers. Glacierized catchments contribute higher proportions of snow and ice melt later in the season as compared to non-glacial streams, fundamentally altering streamflow timing and likely streamflow magnitude. Higher elevation sub-watersheds are more snowmelt dominated throughout the year than low elevation sub-watersheds, which are more rain dominated.

Snowmelt stores water throughout the winter and seasonally contributes to streamflow and aquifer recharge over the course of multiple months (Curran and Biles, 2021; Foks et al., 2018). Groundwater contributes variable volumes of water to streams across elevational gradients, contributing most to low-elevation streams and streams adjacent to large breaks in slope. Seasonally, groundwater proportionally contributes most to streamflow during spring snowmelt and fall rain events. Streamflow may become increasingly driven by groundwater as snow- and ice-melt contributions decrease.

This research informs a general shift from glacierized to deglaciated basins. Although dilute, glaciers export high quantities of phosphorus and labile carbon due to

the high magnitude of flow (Hood and Berner, 2009; Fellman et al., 2014). Fluxes are therefore positively correlated with peak glacier melt, generally in the summer (Fountain and Tangborn, 1985; Curran and Biles, 2021). Snowmelt flushes nutrients stored in soils resulting in a pulse of nitrogen and humic-like carbon in the spring (Foks et al., 2018; Fellman et al., 2014). As glaciers recede and soils develop, the characteristics of nutrients being exported will change, as will the timing. Increasing temperatures are expected to cause less precipitation to fall as snow, snow to melt earlier, more rain on snow events to happen more frequently, and shrubification to occur (Hammond et al., 2019; Musselman et al., 2017; Littell et al., 2018; Dial et al., 2007; Keenan and Riley, 2018). Treeline may shift upwards in elevation as rain contribution continues to increase (Dial et al., 2007; Hammond et al., 2019). The transition of vegetation will alter the water balance through increased transpiration demands. Together, changes in source waters and vegetation will impact streamflow and the transport of sediment and nutrients.

Bedrock Drives Weathering-Derived Solutes

Temperate glaciers alter landscapes by physically weathering underlying bedrock, producing large quantities of silt-sized fresh sediment available for chemical weathering (Hallet et al., 1996; Anderson, 2005). The type of weathering occurring (i.e. carbonate versus silicate) influences the sequestration or release of CO_2 in the atmosphere. My findings show that the type of weathering occurring in the Nellie Juan basin and sub-basins is a mixture of carbonate and silicate weathering. The presence of glaciers does not seem to affect the type of weathering occurring, as both glacial and non-glacial streams exhibit similar geochemical relationships. Additionally, off-glacier streams do not seem to be weathering additional material after passing through the more recently

exposed LIA trimline. Instead, differences in geochemical relationships are driven by underlying bedrock. The proportion of groundwater is positively correlated with the magnitude of weathering-derived solutes, indicating that as groundwater contributes more to streamflow as snow- and ice-melt contribute less, there may be higher fluxes of weathering-derived solutes.

Future Directions

Possible next steps have been identified in multiple parts of this research. In this section, I describe potential future research that builds on this thesis work and discuss planned next steps.

Mixing Model

Chapters 2 and 3 use a three end-member mixing model to determine source water contributions. End members include snow/ice melt, rain, and deep groundwater. Tracers used to distinguish between end members are $\delta^{18}O$ and EC. These end members are not fully representative, as they lack shallow groundwater. Although attempts were made to find a suitable third tracer with our existing dataset, we were limited by our data. Previously collected data were inconsistently analyzed, such that earlier samples were analyzed for a different suite of geochemical tracers than later samples, vastly reducing the number of samples that could be used to determine potential tracers for deep and shallow groundwater. Inconsistencies prevented us from attempting a principal component analysis, which is frequently used in other source water contribution studies (e.g. Wilson et al., 2016; Liu et al., 2004; Frisbee et al., 2011). I would recommend that future samples continue to be analyzed for the same suite of geochemical tracers as recent

samples, including isotopes, major ions, nutrients, and DOC. By doing so, a principal component analysis could be applied to separate shallow and deep groundwater.

I would also recommend updating procedures used to collect shallow and deep groundwater. Current shallow groundwater samples were collected from springs, and should instead be collected using soil lysimeters. This will ensure that we are not collecting shallow overland flow. Deep groundwater would ideally be collected using wells instead of from bedrock seeps. This would prevent possible contamination from algae at the surface of the seeps.

I would also encourage snow sampling to occur throughout the winter season rather than only during freshet. Current snow samples have been isotopically enriched through the preferential melting of lighter isotopes. Sampling after snowmelt has begun results in stream samples with lighter isotopic values than our defined snow end member, which limits the ability of our mixing model to accurately predict stream source water contributions.

Land Cover Classification

Appendix A uses a supervised classification to analyze land cover. The NLCD dataset does not adequately represent land cover in the region, and this method was applied to understand modern land cover. Although the snapshot in time is helpful for contextualizing current influences on streamflow, it cannot be used to measure historic change. The methods used here should be expanded to include more training points and to include historic imagery. Better characterizing historic change can help us better predict shrub encroachment in a rapidly changing landscape. These recommendations will be incorporated into a new project that will characterize the historic (40 year) change

in snow, vegetation, bare ground, and water in the region. The characterization of landscape change can be used to better constrain the influence of land cover on downstream ecosystems.

Weathering Patterns

In Chapter 3 I analyze relationships between ions and nutrients to infer the type of geochemical weathering occurring across glacierized and non-glacial basins. Results vary depending on the relationship examined. When comparing magnesium and calcium concentrations normalized by sodium, samples fell somewhere between values expected from global end-members of silicate and carbonate weathering. Plotting the relationship between bicarbonate and silicate indicated all carbonate weathering. The reason for these differences is unclear but could possibly be explained by the calculation of bicarbonate using the charge balance method. Bicarbonate concentrations could be measured using titration to account for this potential error.

I also recommend that bedrock samples are analyzed using ICP-MS to determine potential mineral differences across the watershed. My results indicate that bedrock likely drives differences in the geochemical signatures of streams, but this could be confirmed with a stronger grasp of lithologic differences.

REFERENCES

Adam, J. C., Hamlet, A. F., & Lettenmaier, D. P. (2009). Implications of global climate change for snowmelt hydrology in the twenty-first century. Hydrological Processes, 23(7), 962–972. https://doi.org/10.1002/hyp.7201

Andermann, C., Longuevergne, L., Bonnet, S., Crave, A., Davy, P., & Gloaguen, R. (2012). Impact of transient groundwater storage on the discharge of Himalayan rivers. Nature Geoscience, 5(2), 127–132. https://doi.org/10.1038/ngeo1356

Anderson, S., Drever, J., & Humphrey, N. (1997). Chemical weathering in glacial environments. Geology, 25(5), 399–402.

Anderson, S. P. (2005). Glaciers show direct linkage between erosion rate and chemical weathering fluxes. Geomorphology, 67(1-2 SPEC. ISS.), 147–157. https://doi.org/10.1016/j.geomorph.2004.07.010

Anderson, S. P., Drever, J. I., Frost, C. D., & Holden, P. (2000). Chemical weathering in the foreland of a retreating glacier.

Armstrong, R. L., Rittger, K., Brodzik, M. J., Racoviteanu, A., Barrett, A. P., Khalsa, S. J. S., Raup, B., Hill, A. F., Khan, A. L., Wilson, A. M., Kayastha, R. B., Fetterer, F., & Armstrong, B. (2019). Runoff from glacier ice and seasonal snow in High Asia: separating melt water sources in river flow. *Regional Environmental Change*, *19*(5), 1249–1261. https://doi.org/10.1007/s10113-018-1429-0

Baraer, M., Mckenzie, J., Mark, B. G., Gordon, R., Bury, J., Condom, T., Gomez, J., Knox, S., & Fortner, S. K. (2015). Contribution of groundwater to the outflow from ungauged glacierized catchments: A multi-site study in the tropical Cordillera Blanca, Peru. *Hydrological Processes*, *29*(11), 2561–2581. https://doi.org/10.1002/hyp.10386

Barnett, T. P., Adam, J. C., & Lettenmaier, D. P. (2005). Potential impacts of a warming climate on water availability in snow-dominated regions. In *Nature* (Vol. 438, Issue 7066, pp. 303–309). Nature Publishing Group. https://doi.org/10.1038/nature04141

Baron, J., & Mast, M. A. (1992). Regional characterization and setting for the Loch Vale watershed study. *Biogeochemistry of a Subalpine Ecosystem: Loch Vale Watershed*, 12-27.

Bergstrom, A., Koch, J. C., O'Neel, S., & Baker, E. (2021). Seasonality of Solute Flux and Water Source Chemistry in a Coastal Glacierized Watershed Undergoing Rapid Change: Wolverine Glacier Watershed, Alaska. *Water Resources Research*, *57*(11). https://doi.org/10.1029/2020WR028725

Beria, H., Larsen, J. R., Ceperley, N. C., Michelon, A., Vennemann, T., & Schaefli, B. (2018). Understanding snow hydrological processes through the lens of stable water isotopes. *Wiley Interdisciplinary Reviews: Water*, *5*(6), 1–23. https://doi.org/10.1002/wat2.1311

Berner, R. A. (2004). *The Phanerozoic carbon cycle: CO2 and O2*. Oxford University Press.

Berner, R., & Maasch, K. (1996). Chemical weathering and controls on atmospheric O2 and CO2: Fundamental principles were enunciated by J.J. Ebelmen in 1845. *Geochimica et Cosmochimica Acta*, *60*(9), 1633–1637.

Blaen, P. J., Hannah, D. M., Brown, L. E., & Milner, A. M. (2014). Water source dynamics of high Arctic river basins. *Hydrological Processes*, *28*(10), 3521–3538. https://doi.org/10.1002/hyp.9891

Bluth, G.J.S. & Kump, L.R. (1994) Lithologic and Climatologic Controls of River Chemistry. Geochimica et Cosmochimica Acta, 58, 2341-2359. https://doi.org/10.1016/0016-7037(94)90015-9

Bouchez, J., & Gaillardet, J. (2014). How accurate are rivers as gauges of chemical denudation of the Earth surface? *Geology*, *42*(2), 171–174. https://doi.org/10.1130/G34934.1

Budyko, M. I. (1974). *Climate and Life.* Academic Press.

Campbell, R. W. (2018). Hydrographic trends in Prince William Sound, Alaska, 1960–2016. *Deep-Sea Research Part II: Topical Studies in Oceanography*, *147*, 43–57. https://doi.org/10.1016/j.dsr2.2017.08.014

Carroll, R. W. H., Bearup, L. A., Brown, W., Dong, W., Bill, M., & Willlams, K. H. (2018). Factors controlling seasonal groundwater and solute flux from snow-dominated basins. *Hydrological Processes*, *32*(14), 2187–2202. https://doi.org/10.1002/hyp.13151

Chiogna, G., Santoni, E., Camin, F., Tonon, A., Majone, B., Trenti, A., & Bellin, A. (2014). Stable isotope characterization of the Vermigliana catchment. *Journal of Hydrology*, *509*, 295–305. https://doi.org/10.1016/j.jhydrol.2013.11.052

Clow, D. W., Schrott, L., Webb, R., Campbell, D. H., Torizzo, A., & Dornblaster, M. (2003). *Ground Water Occurrence and Contributions to Streamflow in an Alpine Catchment, Colorado Front Range Related papers*.

Collins, W. D., Bitz, C. M., Blackmon, M. L., Bonan, G. B., Bretherton, C. S., Carton, J. A., Chang, # Ping, Doney, S. C., Hack, J. J., Henderson, T. B., Kiehl, J. T., Large, W. G., Mckenna, D. S., Santer, B. D., & Smith, R. D. (2006). *The Community Climate System Model Version 3 (CCSM3)*. www.ccsm.ucar.edu/models

Curran, J. H., & Biles, F. E. (2021). Identification of Seasonal Streamflow Regimes and Streamflow Drivers for Daily and Peak Flows in Alaska. *Water Resources Research*, *57*(2). https://doi.org/10.1029/2020WR028425

Dansgaard, W. (1964). Stable isotopes in precipitation. *Tellus*, *16*(4), 436–468. https://doi.org/10.3402/tellusa.v16i4.8993

Denning, A. S., Baron, J., Mast, M. A., & Arthur, M. (1991). Hydrologic pathways and chemical composition of runoff during snowmelt in Loch Vale watershed, Rocky

Mountain National Park, Colorado, USA. *Water, Air, and Soil Pollution*, *59*, 107-123.

Deuerling, K. M., Martin, J. B., Martin, E. E., Abermann, J., Myreng, S. M., Petersen, D., & Rennermalm, Å. K. (2019). Chemical weathering across the western foreland of the Greenland Ice Sheet. *Geochimica et Cosmochimica Acta*, *245*, 426–440. https://doi.org/10.1016/j.gca.2018.11.025

Dial, R. J., Berg, E. E., Timm, K., McMahon, A., & Geek, J. (2007). Changes in the alpine forest-tundra ecotone commensurate with recent warming in southcentral Alaska: Evidence from Orthophotos and field plots. *Journal of Geophysical Research: Biogeosciences*, *112*(4). https://doi.org/10.1029/2007JG000453

Eagleson, P. S. (1978). Climate, soil, and vegetation: 1. Introduction to water balance dynamics. *Water Resources Research*, *14*(5), 705–712. https://doi.org/10.1029/WR014i005p00705

Eiriksdottir, E. S., Gislason, S. R., & Oelkers, E. H. (2013). Does temperature or runoff control the feedback between chemical denudation and climate? Insights from NE Iceland. *Geochimica et Cosmochimica Acta*, *107*, 65–81. https://doi.org/10.1016/j.gca.2012.12.034

Fellman, J. B., Hood, E., Raymond, P. A., Stubbins, A., & Spencer, R. G. M. (2015). Spatial Variation in the Origin of Dissolved Organic Carbon in Snow on the Juneau Icefield, Southeast Alaska. *Environmental Science and Technology*, *49*(19), 11492–11499. https://doi.org/10.1021/acs.est.5b02685

Fetter, C. W. (2001). *Applied Hydrogeology* (4th ed.). Prentice Hall.

Foks, S. S., Stets, E. G., Singha, K., & Clow, D. W. (2018). Influence of climate on alpine stream chemistry and water sources. *Hydrological Processes*, *32*(13), 1993–2008. https://doi.org/10.1002/hyp.13124

Forster, C., & Smith, L. (1988). Groundwater flow systems in mountainous terrain: 2. Controlling factors. *Water Resources Research*, *24*(7), 1011–1023. https://doi.org/10.1029/WR024i007p01011

Foster, G. L., & Vance, D. (2006). Negligible glacial-interglacial variation in continental chemical weathering rates. *Nature*, *444*(7121), 918–921. https://doi.org/10.1038/nature05365

Fountain, A. G., & Tangborn, W. v. (1985). The Effect of Glaciers on Streamflow Variations. In *WATER RESOURCES RESEARCH* (Vol. 21, Issue 4).

Friedman, I., Benson, C., & Gleason, J. (1991). *Stable Isotope Geochemistry: A Tribute to Samuel Epstein Isotopic changes during snow metamorphism*.

Frisbee, M. D., Phillips, F. M., Campbell, A. R., Liu, F., & Sanchez, S. A. (2011). Streamflow generation in a large, alpine watershed in the southern Rocky Mountains of Colorado: Is streamflow generation simply the aggregation of hillslope runoff responses? *Water Resources Research*, *47*(6). https://doi.org/10.1029/2010WR009391

Gaillardet, J., Dupré, B., & All, C. J. (1999). *Geochemistry of large river suspended sediments: Silicate weathering or recycling tracer?*

Gardner, A. S., Moholdt, G., Cogley, J. G., Wouters, B., Arendt, A. A., Wahr, J., Berthier, E., Hock, R., Pfeffer, W. T., Kaser, G., Ligtenberg, S. R. M., Bolch, T., Sharp, M. J., Hagen, J. O., van den Broeke, M. R., & Paul, F. (2013). A Reconciled Estimate of Glacier Contribution to Sea Level Rise: 2003 to 2009. *Science*, *340*(6134), 852–858. https://doi.org/10.1126/science.1234532

Gibbs, M. T., & Kump, L. R. (1994). Global chemical erosion during the Last Glacial Maximum and the present: Sensitivity to changes in lithology and hydrology. *Paleoceanography*, *9*(4), 529–543. https://doi.org/10.1029/94PA01009

Gleick, P. H., & Palaniappan, M. (2010). Peak water limits to freshwater withdrawal and use. *Proceedings of the National Academy of Sciences of the United States of America*, *107*(25), 11155–11162. https://doi.org/10.1073/pnas.1004812107

Gröning, M., Lutz, H. O., Roller-Lutz, Z., Kralik, M., Gourcy, L., & Pöltenstein, L. (2012). A simple rain collector preventing water re-evaporation dedicated for δ 18O and δ 2H analysis of cumulative precipitation samples. *Journal of Hydrology*, *448–449*, 195–200. https://doi.org/10.1016/j.jhydrol.2012.04.041

Haldorsen, S. (1981). Grain-size distribution of subglacial till and its relation to glacial crushing and abrasion. *Boreas*, *10*, 91–105.

Hallet, B., Hunter, L., & Bogen, J. (1996). Rates of erosion and sediment evacuation by glaciers: A review of field data and their implications. *Global and Planetary Change*, *12*(1–4), 213–235. https://doi.org/10.1016/0921-8181(95)00021-6

Hammond, J. C., Harpold, A. A., Weiss, S., & Kampf, S. K. (2019). Partitioning snowmelt and rainfall in the critical zone: Effects of climate type and soil properties. *Hydrology and Earth System Sciences*, *23*(9), 3553–3570. https://doi.org/10.5194/hess-23-3553-2019

Hannah, D. M., Gurnell, A. M., & McGregor, G. R. (2000). Spatio-temporal variation in microclimate, the surface energy balance and ablation over a cirque glacier. *International Journal of Climatology*, *20*(7), 733–758. https://doi.org/10.1002/1097-0088(20000615)20:7<733::AID-JOC490>3.0.CO;2-F

Hayashi, M. (2020). Alpine Hydrogeology: The Critical Role of Groundwater in Sourcing the Headwaters of the World. *Groundwater*, *58*(4), 498–510. https://doi.org/10.1111/gwat.12965

Herman, F., Seward, D., Valla, P. G., Carter, A., Kohn, B., Willett, S. D., & Ehlers, T. A. (2013). Worldwide acceleration of mountain erosion under a cooling climate. *Nature*, *504*(7480), 423–426. https://doi.org/10.1038/nature12877

Hock, R. (2005). Glacier melt: A review of processes and their modelling. In *Progress in Physical Geography* (Vol. 29, Issue 3, pp. 362–391). https://doi.org/10.1191/0309133305pp453ra

Holdridge, L. R. (1967). *Life zone ecology*.

Hood, E., & Berner, L. (2009). Effects of changing glacial coverage on the physical and biogeochemical properties of coastal streams in southeastern Alaska. *Journal of Geophysical Research: Biogeosciences*, *114*(3). https://doi.org/10.1029/2009JG000971

Hood, E., & Scott, D. (2008). Riverine organic matter and nutrients insoutheast Alaska affected by glacial coverage. *Nature Geoscience*, *1*(9), 583–587. https://doi.org/10.1038/ngeo280

Hugonnet, R., McNabb, R., Berthier, E., Menounos, B., Nuth, C., Girod, L., Farinotti, D., Huss, M., Dussaillant, I., Brun, F., & Kääb, A. (2021). Accelerated global glacier mass loss in the early twenty-first century. *Nature*, *592*(7856), 726–731. https://doi.org/10.1038/s41586-021-03436-z

Huss, M., Hock, R. Global-scale hydrological response to future glacier mass loss. *Nature Clim Change* **8**, 135–140 (2018). https://doi.org/10.1038/s41558-017-0049-x

Ibarra, D. E., Caves, J. K., Moon, S., Thomas, D. L., Hartmann, J., Chamberlain, C. P., & Maher, K. (2016). Differential weathering of basaltic and granitic catchments from concentration–discharge relationships. *Geochimica et Cosmochimica Acta*, *190*, 265–293. https://doi.org/10.1016/j.gca.2016.07.006

Jenckes, J., Ibarra, D. E., & Munk, L. A. (2022). Concentration-Discharge Patterns Across the Gulf of Alaska Reveal Geomorphological and Glacierization Controls on Stream Water Solute Generation and Export. In *Geophysical Research Letters* (Vol. 49, Issue 1). John Wiley and Sons Inc. https://doi.org/10.1029/2021GL095152

Kampf, S., Markus, J., Heath, J., & Moore, C. (2015). Snowmelt runoff and soil moisture dynamics on steep subalpine hillslopes. *Hydrological Processes*, *29*(5), 712–723. https://doi.org/10.1002/hyp.10179

Keenan, T. F., & Riley, W. J. (2018). Greening of the land surface in the world's cold regions consistent with recent warming. In *Nature Climate Change* (Vol. 8, Issue 9, pp. 825–828). Nature Publishing Group. https://doi.org/10.1038/s41558-018-0258-y

Klaar, M. J., Kidd, C., Malone, E., Bartlett, R., Pinay, G., Chapin, F. S., & Milner, A. (2015). Vegetation succession in deglaciated landscapes: Implications for

sediment and landscape stability. *Earth Surface Processes and Landforms*, *40*(8), 1088–1100. https://doi.org/10.1002/esp.3691

Kneib, M., Cauvy-Fraunié, S., Escoffier, N., Boix Canadell, M., Horgby, & Battin, T. J. (2020). Glacier retreat changes diurnal variation intensity and frequency of hydrologic variables in Alpine and Andean streams. *Journal of Hydrology*, *583*. https://doi.org/10.1016/j.jhydrol.2020.124578

Koch, J. C., Baker, E. H., Bergstrom, A., O'Neel, S. R., Myers, K. and Sawicki, S., 2021, Geochemistry of water sources in the Wolverine Glacier Watershed, Alaska in 2016 and 2017: U.S. Geological Survey data release, https://doi.org/10.5066/P9LLXNAX.

Koch, J. C., Kikuchi, C. P., Wickland, K. P., & Schuster, P. (2014). Runoff sources and flow paths in a partially burned, upland boreal catchment underlain by permafrost. *Water Resources Research*, *50*(10), 8141–8158. https://doi.org/10.1002/2014WR015586

Kump, L. R., Arthur, M. A., Patzkowsky, M. E., Gibbs, M. T., Pinkus, D. S., & Sheehan, P. M. (1999). A weathering hypothesis for glaciation at high atmospheric pCO 2 during the Late Ordovician. In *Palaeogeography, Palaeoclimatology, Palaeoecology* (Vol. 152).

Littell, J. S., McAfee, S. A., & Hayward, G. D. (2018). Alaska snowpack response to climate change: Statewide snowfall equivalent and snowpack water scenarios. *Water (Switzerland)*, *10*(5). https://doi.org/10.3390/w10050668

Liu, Z., Dreybrodt, W., & Liu, H. (2011). Atmospheric CO2 sink: Silicate weathering or carbonate weathering? *Applied Geochemistry*, *26*(SUPPL.). https://doi.org/10.1016/j.apgeochem.2011.03.085

Liu, F., Williams, M. W., & Caine, N. (2004). Source waters and flow paths in an alpine catchment, Colorado Front Range, United States. *Water Resources Research*, *40*(9). https://doi.org/10.1029/2004WR003076

Lundquist, J. D., Cayan, D. R., & Dettinger, M. D. (2004). *Spring Onset in the Sierra Nevada: When Is Snowmelt Independent of Elevation?* http://www.solinst.com

Maher, K. (2011). The role of fluid residence time and topographic scales in determining chemical fluxes from landscapes. *Earth and Planetary Science Letters*, *312*(1–2), 48–58. https://doi.org/10.1016/j.epsl.2011.09.040

Markovich, K. H., Maxwell, R. M., & Fogg, G. E. (2016). Hydrogeological response to climate change in alpine hillslopes. *Hydrological Processes*, *30*(18), 3126–3138. https://doi.org/10.1002/hyp.10851

McAfee, S., Guentchev, G., & Eischeid, J. (2014). Reconciling precipitation trends in Alaska: 2. gridded data analyses. *Journal of Geophysical Research*, *119*(22), 13820–13837. https://doi.org/10.1002/2014JD022461

McGuire, K. J., & McDonnell, J. J. (2006). A review and evaluation of catchment transit time modeling. *Journal of Hydrology*, *330*(3–4), 543–563. https://doi.org/10.1016/j.jhydrol.2006.04.020

Milner, A. M., Khamis, K., Battin, T. J., Brittain, J. E., Barrand, N. E., Füreder, L., Cauvy-Frauní, S., Ar Gíslason, M. ´, Jacobsen, D., Hannah, D. M., Hodson, A. J., Hood, E., Lencioni, V., Olafsson, S. ´, Robinson, C. T., Tranter, M., & Brown, L. E. (2017). Glacier shrinkage driving global changes in downstream systems. *PNAS*, *114*(37), 9770–9778. https://doi.org/10.1073/pnas.1619807114/-/DCSupplemental

Milner, A. M., Brown, L. E., & Hannah, D. M. (2009). Hydroecological response of river systems to shrinking glaciers. In *Hydrological Processes* (Vol. 23, Issue 1, pp. 62–77). https://doi.org/10.1002/hyp.7197

Moser, H., & Stichler, W. (1980). Environmental isotopes in ice and snow. *Handbook of Environmental Isotope Geochemistry*, *1*.

Mote, P. W., Hamlet, A. F., Clark, M. P., & Lettenmaier, D. P. (2005). Declining mountain snowpack in western north America. *Bulletin of the American Meteorological Society*, *86*(1), 39–49. https://doi.org/10.1175/BAMS-86-1-39

Musselman, K. N., Clark, M. P., Liu, C., Ikeda, K., & Rasmussen, R. (2017). Slower snowmelt in a warmer world. *Nature Climate Change*, *7*(3), 214–219. https://doi.org/10.1038/nclimate3225

O'Neel, S., Hood, E., Bidlack, A. L., Fleming, S. W., Arimitsu, M. L., Arendt, A., Burgess, E., Sergeant, C. J., Beaudreau, A. H., Timm, K., Hayward, G. D., Reynolds, J. H., & Pyare, S. (2015). Icefield-to-ocean linkages across the northern pacific coastal temperate rainforest ecosystem. *BioScience*, *65*(5), 499–512. https://doi.org/10.1093/biosci/biv027

O'Neel, S., Hood, E., Arendt, A., & Sass, L. (2014). Assessing streamflow sensitivity to variations in glacier mass balance. *Climatic Change*, *123*(2), 329–341. https://doi.org/10.1007/s10584-013-1042-7

Raiswell, R. (1984). CHEMICAL MODELS OF SOLUTE ACQUISITION IN GLACIAL MELT WATERS. In *JournaL of GLaoioLogy*> (Vol. 30, Issue 4).

Ryu, J. S., & Jacobson, A. D. (2012). CO 2 evasion from the Greenland Ice Sheet: A new carbon-climate feedback. *Chemical Geology*, *320–321*, 80–95. https://doi.org/10.1016/j.chemgeo.2012.05.024

Scribner, C. A., Martin, E. E., Martin, J. B., Deuerling, K. M., Collazo, D. F., & Marshall, A. T. (2015). Exposure age and climate controls on weathering in deglaciated watersheds of western Greenland. *Geochimica et Cosmochimica Acta*, *170*, 157–172. https://doi.org/10.1016/j.gca.2015.08.008

Somers, L. D., McKenzie, J. M., Mark, B. G., Lagos, P., Ng, G. H. C., Wickert, A. D., Yarleque, C., Baraër, M., & Silva, Y. (2019). Groundwater Buffers Decreasing Glacier Melt in an Andean Watershed—But Not Forever. *Geophysical Research Letters*, *46*(22), 13016–13026. https://doi.org/10.1029/2019GL084730

Stephenson, N. L. (1990). Climatic control of vegetation distribution: The role of the water balance. In *Am. Nat* (Vol. 135, Issue 5).

Stumm, W., & Morgan, J. J. (2012). *Aquatic chemistry: chemical equilibria and rates in natural waters*. John Wiley & Sons.

Sturm, M., Mcfadden, J. P., Liston, G. E., Stuart Chapin Iii, # F, Racine, C. H., & Holmgren, J. (2001). Snow-Shrub Interactions in Arctic Tundra: A Hypothesis with Climatic Implications.

Tague, C., Grant, G., Farrell, M., Choate, J., & Jefferson, A. (2008). Deep groundwater mediates streamflow response to climate warming in the Oregon Cascades. *Climatic Change*, *86*(1–2), 189–210. https://doi.org/10.1007/s10584-007-9294-8

Taylor, R. G., Scanlon, B., Döll, P., Rodell, M., van Beek, R., Longuevergne, L., LeBlanc, M., Famiglietti, J. S., Edmunds, M., Konikow, L., Green, T., Chen, J., Taniguchi, M., Bierkens, M. F., MacDonald, A., Fan, Y., Maxwell, R., Yechieli, Y., Gurdak, J., … Holman, I. (2013). Groundwater and climate change: recent advances and a look forward. *Nature Climate Change*, 322–329.

Tedrow, J. C. F., & Harries, H. (1960). Tundra Soil in Relation to Vegetation, Permafrost and Glaciation. In *Source: Oikos* (Vol. 11, Issue 2). https://about.jstor.org/terms

Torres, M. A., Moosdorf, N., Hartmann, J., Adkins, J. F., & West, A. J. (2017). Glacial weathering, sulfide oxidation, and global carbon cycle feedbacks. *Proceedings of the National Academy of Sciences of the United States of America*, *114*(33), 8716–8721. https://doi.org/10.1073/pnas.1702953114

Tóth, J. (1963). A theoretical analysis of groundwater flow in small drainage basins. *Journal of Geophysical Research*, *68*(16), 4795–4812. https://doi.org/10.1029/jz068i016p04795

Tranter, M., Huybrechts, P., Munhoven, G., Sharp, M. J., Brown, G. H., Jones, I. W., Hodson, A. J., Hodgkins, R., & Wadham, J. L. (2002). *Direct effect of ice sheets on terrestrial bicarbonate, sulphate and base cation fluxes during the last glacial cycle: minimal impact on atmospheric CO 2 concentrations*. www.elsevier.com/locate/chemgeo

van Patten, D. J. (2000). *Soil Survey of Lower Kenai Peninsula Area, Alaska*. http://www.nrcs.usda.gov

Vaughn, B. H., & Fountain, A. G. (2005). *Stable isotopes and electrical conductivity as keys to understanding water pathways and storage in South Cascade Glacier, Washington, USA*. https://www.cambridge.org/core.

Viviroli, D., Dürr, H. H., Messerli, B., Meybeck, M., & Weingartner, R. (2007). Mountains of the world, water towers for humanity: Typology, mapping, and

global significance. *Water Resources Research*, *43*(7). https://doi.org/10.1029/2006WR005653

Wadham, J. L., Cooper, R. J., Tranter, M., & Hodgkins, R. (2001). *Enhancement of glacial solute fluxes in the proglacial zone of a polythermal glacier*.

Walker, J. C. G., Hays, P. B., & Kasting, J. F. (1981). A negative feedback mechanism for the long-term stabilization of Earth's surface temperature. *Journal of Geophysical Research*, *86*(C10), 9776–9782. https://doi.org/10.1029/JC086iC10p09776

Walsh, J. E., & Brettschneider, B. (2019). Attribution of recent warming in Alaska. *Polar Science*, *21*, 101–109. https://doi.org/10.1016/j.polar.2018.09.002

White, A. F., & Brantley, S. L. (2003). The effect of time on the weathering of silicate minerals: Why do weathering rates differ in the laboratory and field? *Chemical Geology*, *202*(3–4), 479–506. https://doi.org/10.1016/j.chemgeo.2003.03.001

White, A. F., Bullen, T. D., Vivit, D. v, Schulz, M. S., & Clow, D. W. (1999). *The role of disseminated calcite in the chemical weathering of granitoid rocks*.

Wilson, A. M., Williams, M. W., Kayastha, R. B., & Racoviteanu, A. (2016). Use of a hydrologic mixing model to examine the roles of meltwater, precipitation and groundwater in the Langtang River basin, Nepal. *Annals of Glaciology*, *57*(71), 155–168. https://doi.org/10.3189/2016aog71a067

Wilson, F. H., & Hults, C. P. (2012). *Geology of the Prince William Sound and Kenai Peninsula Region, Alaska Including the Kenai, Seldovia, Seward, Blying Sound, Cordova, and Middleton Island 1:250,000-scale quadrangles*.

Wimpenny, J., Burton, K. W., James, R. H., Gannoun, A., Mokadem, F., & Gíslason, S. R. (2011). The behaviour of magnesium and its isotopes during glacial weathering in an ancient shield terrain in West Greenland. *Earth and Planetary Science Letters*, *304*(1–2), 260–269. https://doi.org/10.1016/j.epsl.2011.02.008

Winnick, M. J., & Maher, K. (2018). Relationships between CO2, thermodynamic limits on silicate weathering, and the strength of the silicate weathering feedback. *Earth*

and Planetary Science Letters, *485*, 111–120. https://doi.org/10.1016/j.epsl.2018.01.005

YSI. (2017). *EcoSense EC300: User Manual.* Retrieved from https://www.ysi.com/File%20Library/Documents/Manuals/YSI-EC300A-EC300M-Manual-English.pdf.

APPENDIX A

Supervised Land Cover Classification

A.1 Landsat Imagery Acquisition and Classification Model

To characterize land cover in the Nellie Juan basin and its sub-watersheds, I performed a supervised classification of land cover. I used a 30x30m resolution Landsat 8 image acquired on August 29th, 2021 (citation for landsat), the most recent cloud and snow free image, allowing for maximum likelihood of accurate vegetation classification. Training points were manually chosen using Maxar satellite imagery acquired on September 11th, 2021 at 0.5 m-resolution, accessed through ESRI World Imagery (cite). Seventy points were each assigned to five land cover types: forest, shrub, tundra, snow and ice, and rock/water. Eighty percent of the points were used to train a model that extracted the reflectance values at each point from Landsat bands 1-7. Land cover was then predicted across the region using a model developed by a recursive partitioning of a classification tree in the rpart package (v.4.1.19; Therneau et al., 2022). The remaining twenty percent of points were used as a testing dataset. The model accuracy was assessed using a confusion matrix in the caret package (v.6.0.93; Kuhn, 2022).

A.2 Supervised Classification Maps and Assessment

Sub-watersheds were chosen based on on-the-ground and aerial observations of land cover coupled with ease of access. The results of the land cover classification show that some sub-watersheds primarily drain areas covered by a single land cover class, while others are more mixed in land cover than inferred from field observations. For example, Tundra Stream drains an area primarily covered by tundra vegetation (85%) followed by rock and water (10%) and Forest Stream drains a basin completely covered

by forest (100%) (Figures A.1 and 2.3). Shrub Creek, however, drains a basin only partially covered by shrubs (16%), while the primary cover is tundra vegetation (80%) (Figure 2.8). The performance of the model was assessed using a confusion matrix. The accuracy of the model was 95.5% with a kappa value of 0.94.

Land cover misclassifications most often occurred in the prediction of rock/water and tundra, likely due to the similarities between their reflectance values in bands 1-4. The mixed pixel effect in the 30 m-resolution of Landsat imagery may be particularly problematic for tundra and bare rock, which are observed in intermixed patches in the field. Visual inspection of the classification maps also indicates that rock is often misclassified as forest around glacier margins, potentially do to the semi-persistent shadowing near the glacier margins (Figure A.2). Although the spatial resolution of this analysis is likely insufficient for fine scale analysis, it seems to suitably represent land cover at the basin scale.

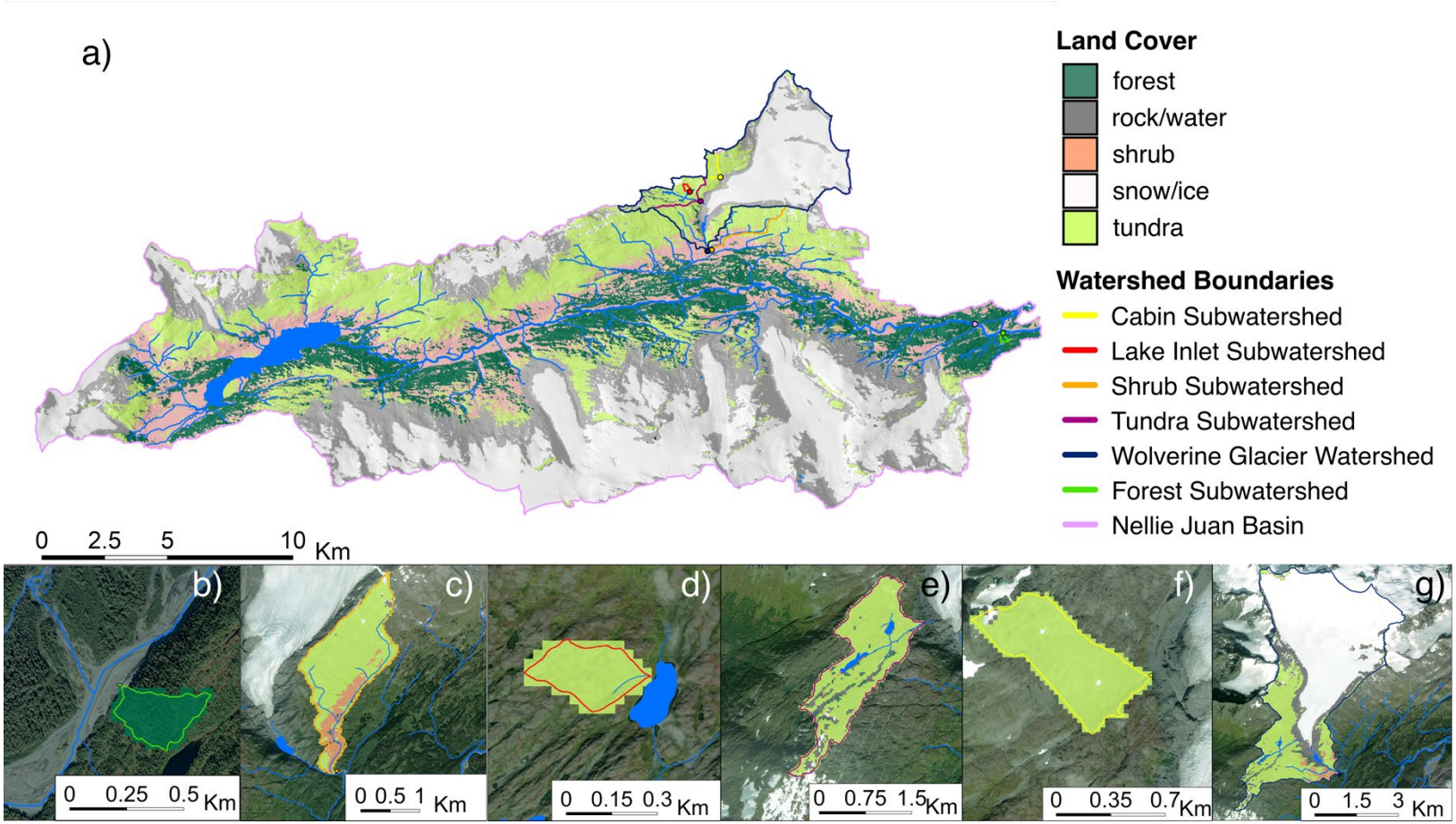

Figure A.1 Land cover classification results from a supervised classification. Inset map a) shows the entire Nellie Juan basin with sub-watershed outlines. Inset b) shows the Forest watershed, c) Shrub Creek, d) Lake Inlet, e) Tundra Stream, f) Cabin Stream, and g) the Wolverine Glacier watershed.

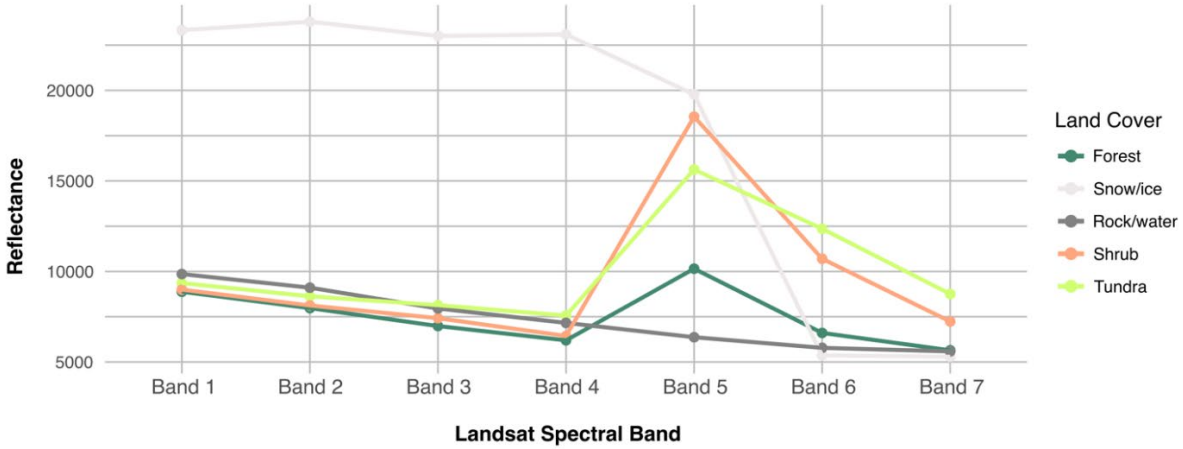

Figure A.2 Landsat spectral band profile for each land cover type.